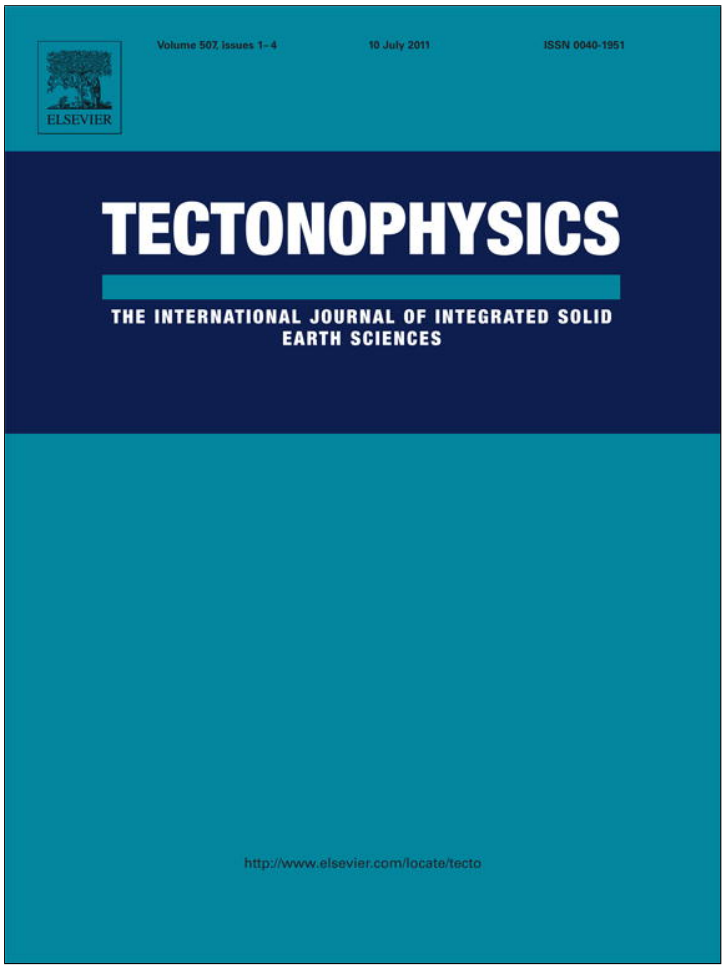

Tectonophysics 507 (2011) 31–46

Contents lists available at ScienceDirect

Tectonophysics

journal homepage: www.elsevier.com/locate/tecto

Orocline timing through joint analysis: Insights from the Ibero-Armorican Arc

Daniel Pastor-Galán [a,*], Gabriel Gutiérrez-Alonso [a], Arlo Brandon Weil [b]

[a] Departamento de Geología, Universidad de Salamanca, Plaza de los Caídos s/n, 37008 Salamanca, Spain
[b] Department of Geology, Bryn Mawr College, Bryn Mawr, PA 19010, USA

ARTICLE INFO

Article history:
Received 13 December 2010
Received in revised form 13 May 2011
Accepted 16 May 2011
Available online 26 May 2011

Keywords:
Orocline
Orocline timing
Joint analysis
Ibero-Armorican arc
Cantabrian–Asturian arc

ABSTRACT

The timing and kinematics of oroclinal bending in the core of the Ibero-Armorican Arc (IAA) has recently been constrained using paleomagnetic data from the Cantabrian Zone in northern Iberia. This study analyzes the joint-patterns present in rock units deposited pre-, syn- and post-oroclinal bending. Systematic changes in the orientations of tensional joint-sets in superimposed stratigraphic units are interpreted to record the progressive stages of oroclinal bending in the core of the IAA. Time constrains for joint set development are constrained by the known ages of the bounding unconformities that limit the studied stratigraphic units. Joint azimuth variability in the pre-orocline rocks (Neoproterozoic to pre-Upper Carboniferous) is comparable to the present arc curvature of the orocline (about 180°); the joints in the syn-orocline rocks (Upper Pennsylvanian or Stephanian, 304 to 299 Ma) show a lower azimuthal variability that is comparable to about 50–70% of the total curvature seen in pre-orocline rocks. Finally, post-orocline rocks (Permian) contain joints that have uniform azimuths for each set across the entirety of the present-day arc. Together these spatially and temporally distinct joint sets suggest that rotations in the Cantabrian Zone took place in the Upper Pennsylvanian during a ca. 10 Ma time period, which agrees well with previous paleomagnetic arguments. The data also provides supporting evidence for oroclinal bending by rotation around vertical axes of an initially linear, or nearly linear, orogenic belt. And finally, these data highlight the potential power in using tectonic joint sets for constraining thrust belt kinematics in curved orogenic systems when unconformity bounded stratigraphic sequences are present that are coeval with orocline development.

1. Introduction

Understanding the stress and strain fields associated with secondarily bent orogens has been the focus of considerable debate since S.W. Carey originally proposed the idea of an orocline in 1955 (e.g., Irving and Opdyke, 1965; Lowrie and Hirt, 1986; Muttoni et al., 1998; Van der Voo and Channell, 1980; Weil and Sussman, 2004). Carey defined an orocline (Carey, 1955) as an "orogenic system that has been flexed in plan-view to a horse-shoe or elbow shape" meaning that they were originally linear belts that have bent around a vertical-axis subsequent to the main orogenic episode and can be considered as secondary arcs (Eldredge et al., 1985; Weil et al., 2010). In contrast, primary arcs constitute orogenic belts that were originally curved and whose formation did not involve secondary rotation. Progressive arcs are those curved belts that undergo some rotation during initial orogeny, or those belts that start with a primary curvature and are later tightened during subsequent deformation (Weil and Sussman, 2004). Classifying curved orogens is, therefore, difficult, and requires recognition of the deformation phases involved in their formation. To distinguish between primary and progressive arcs, two deformation stages need to be identified: an initial compressive phase that produces a linear orogenic belt, and a second phase that results in vertical-axis rotation (Weil and Sussman, 2004). Several models for the development of bent orogens have been proposed. Some authors have proposed thin-skinned tectonic mechanisms for oroclinal bending (Eldredge et al., 1985; Marshak, 1988, Marshak, 2004; Marshak and Tabor, 1989; Macedo and Marshak, 1999) where only the uppermost crust is involved. Alternatively, some oroclines are described as thick-skinned features that involve the entire lithosphere (Gutiérrez-Alonso et al., 2004, 2008; Johnston, 2001) and can be an important process during the final stages of, or immediately after, orogeny.

One of the most spectacular curved orogenic systems on Earth is the Cantabrian–Asturian Arc (CAA), which defines the inner-core of the larger Ibero-Armorican Arc (IAA) (Brun and Burg, 1982), and today traces 180° of structural trend (Weil et al., 2001) (Fig. 1). Exposed Paleozoic strata within the CAA were deposited along the northern margin of Gondwana, forming the southern passive margin of the Rheic Ocean (Martínez-Catalán, 2002; Murphy et al., 2006). During the Variscan orogeny these strata were imbricated, forming a classic foreland fold–thrust belt. The thrusts in the CAA have a concave geometry towards the foreland and a thrust propagation direction towards the core of the arc (Pérez-Estaún et al., 1988). In addition to thrusts, and geometrically linked to their frontal ramps, a longitudinal,

* Corresponding author. Tel.: +34 923294488.
E-mail address: dpastorgalan@usal.es (D. Pastor-Galán).

0040-1951/$ – see front matter © 2011 Elsevier B.V. All rights reserved.
doi:10.1016/j.tecto.2011.05.005

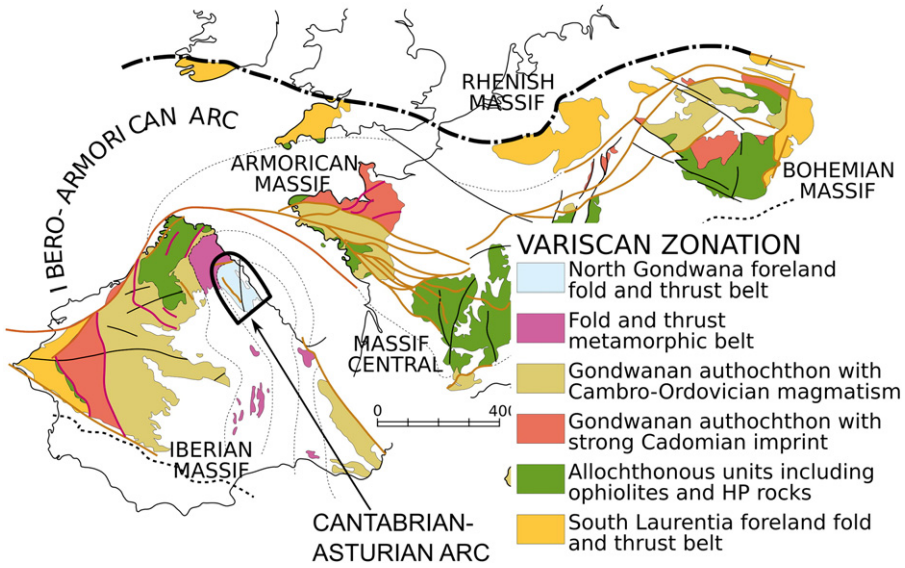

Fig. 1. Tectono-stratigraphic zonation of the Western European Variscan Belt (modified from Martínez-Catalán et al., 2007) showing the overall trace of the Ibero-Armorican Arc and the location of the Cantabrian–Asturian Arc (Fig. 3).

arc-parallel set of fault-bend folds is identified. Subsequent to thrust initiation and their related structures, a younger arc-perpendicular radial fold set (Julivert and Marcos, 1973) developed, which resulted in thrust sheet folding and formation of complex interference patterns imposed on existing fault-bend folds. Some of the aforementioned radial folds nucleated on tear faults or existing folds associated with lateral ramps of existing thrusts (Aller and Gallastegui, 1995; Alvarez-Marron and Perez-Estaun, 1988; Weil, 2006).

There are multiple structural and tectonic studies of the IAA that focus on understanding the kinematics and origin of its arcuate shape.

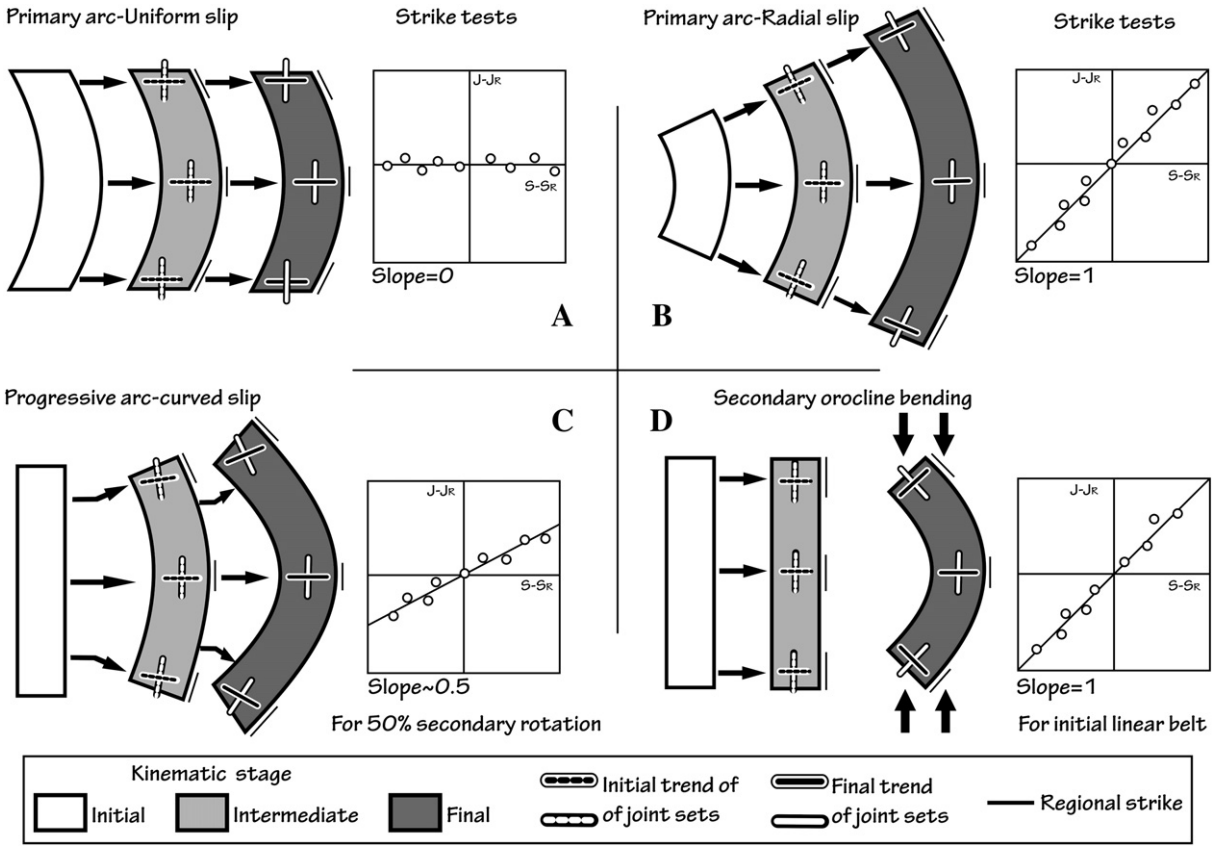

Fig. 2. Idealized kinematic models for curved orogenic belts (modified from Yonkee and Weil, 2010a). Joint sets parallel and normal to the fold axes and regional strike are indicated for initial, intermediate and final stages of deformation. Corresponding strike-test plots for each joint set depict the expected slope for each model. A slope of one is expected for primary arcs with radial slip and secondary arcs (oroclines), slopes between 0 and 1 are expected for progressive arcs (the sooner the joint sets are developed the closer to 1 will be the slope) and slopes of 0 are expected for primary arcs with uniform slip.

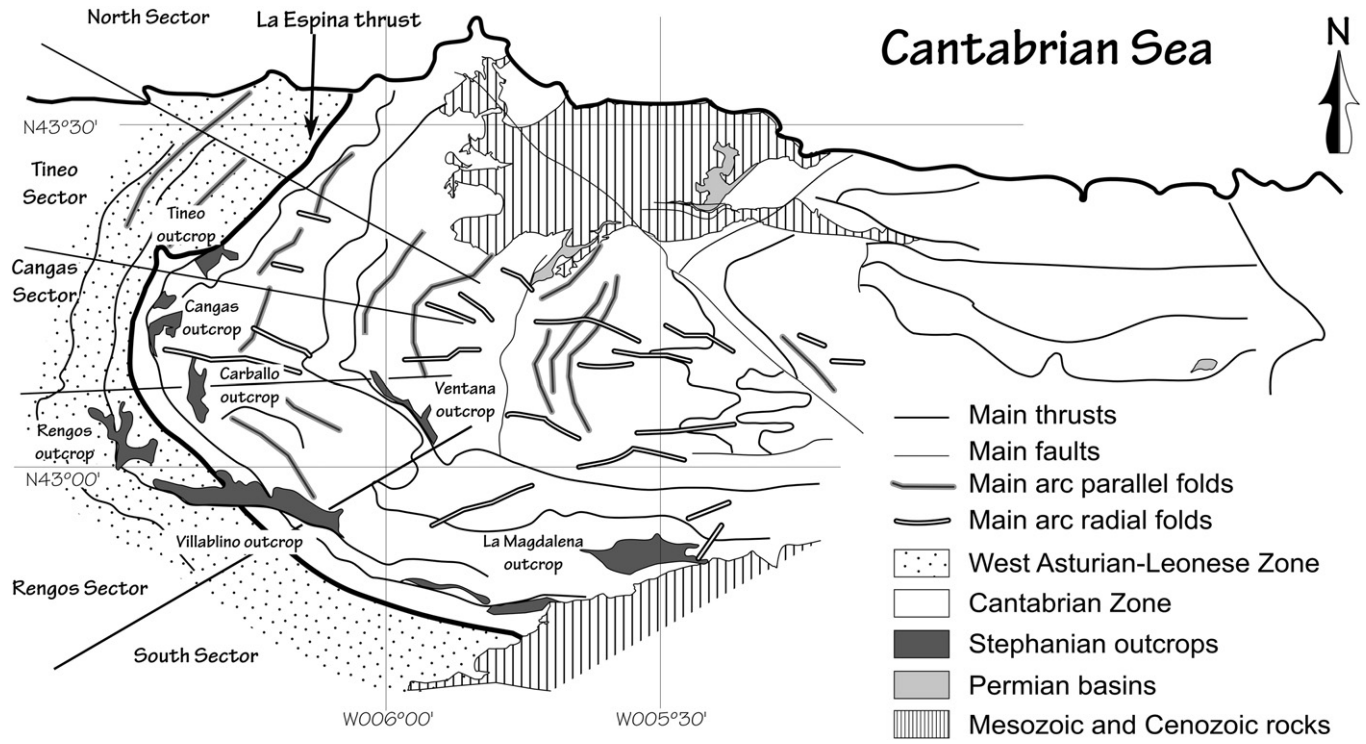

Fig. 3. Simplified map of the Cantabrian–Asturian Arc, showing the pre-Stephanian rocks in the Cantabrian Zone and West Asturian–Leonese Zone, the unconformably overlying Stephanian outcrops and the Permian basins.

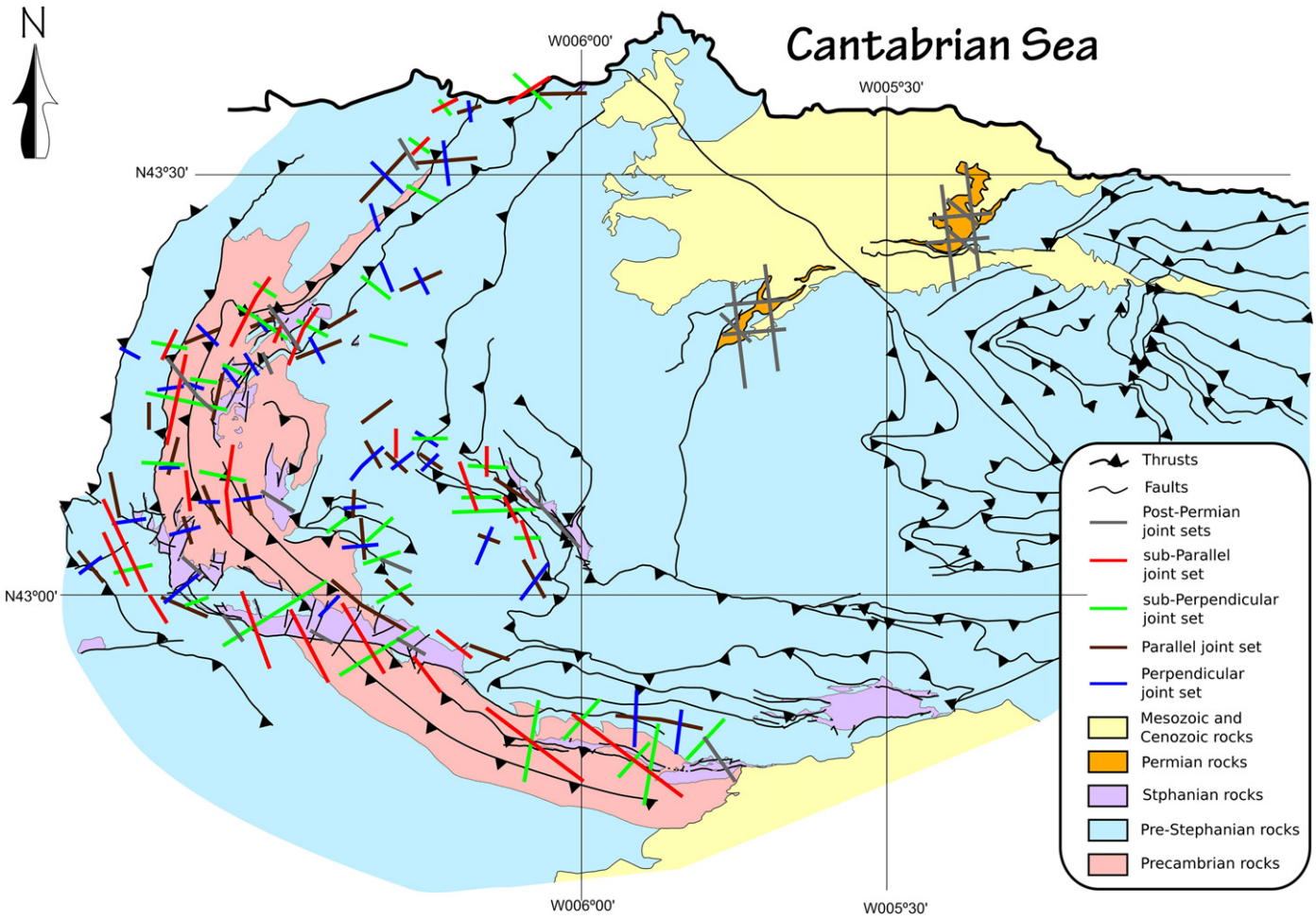

Fig. 4. Geological map plotting all the different joint sets described in the text.

Models explaining IAA curvature include: (i) a primary arc inherited from a Neoproterozoic embayment (Lefort, 1979); (ii) a progressive arc resulting from the indentation of a point shaped continental block (Brun and Burg, 1982; Ribeiro et al., 1995), a non-cylindrical collision (Martínez-Catalán, 1990), or a thin-skinned origin with a progressive change in thrust transport direction (i.e., the photographic iris model of Pérez-Estaún et al., 1988); or (iii) a true orocline formed by the rotation around a vertical-axis of an originally linear orogen (e.g., Weil et al., 2000, 2010). The latter model relies on structural and paleomagnetic data (Kollmeier et al., 2000; Pares et al., 1994; Weil et al., 2000, 2001, 2010) and implies that early longitudinal thrusts and related folds formed due to east–west shortening (in present-day coordinates) (i.e., Pérez-Estaún et al., 1991), which produced a linear north–south trending fold–thrust belt. Subsequently, north–south shortening (Julivert and Marcos, 1973; Weil et al., 2001) occurred in the uppermost Carboniferous–earliest Permian (Merino-Tomé et al., 2009; Rodríguez-Fernández and Heredia, 1990; Weil et al., 2010), which resulted in large-scale crustal rotations that produced the curved arc seen today. These observations suggest that the IAA is a true orocline in which vertical-axis rotations of an originally linear belt was caused by a dramatic change in the plate-scale stress field from east–west to north–south (in present-day coordinates) during the final stages of Pangea amalgamation (Gutiérrez-Alonso et al., 2008). Given the scale of the IAA, of which the CAA occupies its inner core, and the coeval lithospheric-scale response under Iberia (e.g., lithospheric delamination and mantle replacement (Fernandez-Suarez et al., 1998; Gutiérrez-Alonso et al., 2004, 2011), the IAA has been recently interpreted as a thick-skinned orocline. This interpretation is in contrast to other curved mountain belts that developed in foreland fold–thrust belt systems without an associated lithospheric response (Marshak, 2004).

In order to further test and constrain the predicted stress field change that caused oroclinal bending, we have analyzed the spatial and temporal distribution of systematic tensile joints from multiple rock units exposed around the arc of the CAA. Despite the cautions needed in interpreting joint systems as kinematic markers in polydeformed rock volumes associated with compressional tectonic regimes, joint sets do provide a sensitive record of the syn-kinematic stress field at the time of deformation (Whitaker and Engelder, 2005). This is especially true when there are angular unconformities that constrain multiple tectonic pulses and/or events. Previous studies have demonstrably shown that well-developed tectonic joint sets can serve as a robust proxy for the orientation of the lithospheric-scale stress field (e.g., Whitaker and Engelder, 2006): for example, from studies in the Ouachita salient (Whitaker and Engelder, 2006), the Appalachian plateau (Engelder and Geiser, 1980), the Idaho–Wyoming salient (Yonkee and Weil, 2010a), the Variscan belt in Wales (Dunne and North, 1990), and the Pyrenees (Turner and Hancock, 1990). In some regions joint patterns may record a cumulative deformation history, and consequently the rocks may record several systematic joint sets caused by temporally distinct stress fields, which produce a succession of tensile fracture development. Thus, when multiple joint sets are present, caution is needed in using the spatial pattern of joints across a region to interpret tectonic history (Dunne and North, 1990; Engelder and Geiser, 1980). In short, as tectonic complexity increases, it becomes more difficult to understand systematic joint patterns, and thus interpret if they are controlled by changes in the regional or local stress field (Fischer and Jackson, 1999).

One way to unravel the regional development of successive joint sets is to study their occurrence in sequences where the presence of angular unconformities constrains the timing of joint formation into pre- and post-unconformity sets. From this point of view, if a joint set is only developed in an older rock sequence, and is not present in rocks that overly an unconformity, it can be assumed that the joint set developed prior to deposition of the post-unconformity rocks. If subsequent tectonic events affect the entire rock sequence, new joint sets can be superposed onto the lower and upper rock sequences that allow constraints to be placed on the relative timing of joint formation. Joint sets in the CAA region are preserved in a syn-orogenic Carboniferous succession, which contains angular unconformities that bracket the age of orocline development, thus providing an ideal opportunity to bracket the timing of oroclinal bending using joints as stress markers during progressive deformation.

This study catalogs the systematic joint sets present in the core of the IAA in order to characterize the tectonic history, and constrain the timing of changes in the stress field responsible for oroclinal bending. To achieve this, a complete census of systematic joint sets was performed in three groups of sedimentary rocks that are currently separated by angular unconformities, and are constrained to predate, to be coeval with, and to postdate orocline formation. Subsequent to orientation analysis, data from the three rock groups were analyzed using a strike tests to quantitatively evaluate the relative timing of joint formation with respect to thrust trace modification.

The strike test (also called an orocline test) (Eldredge et al., 1985; Schwartz and Van der Voo, 1983) evaluates the relationship between changes in regional structural trend (relative to a reference trend), and the orientations of a given geologic fabric element (e.g., fractures, cleavage, veins, lineations, paleomagnetic declination, etc.). This methodology has been mainly used by paleomagnetists (e.g., Schwartz and Van der Voo, 1983; Weil and

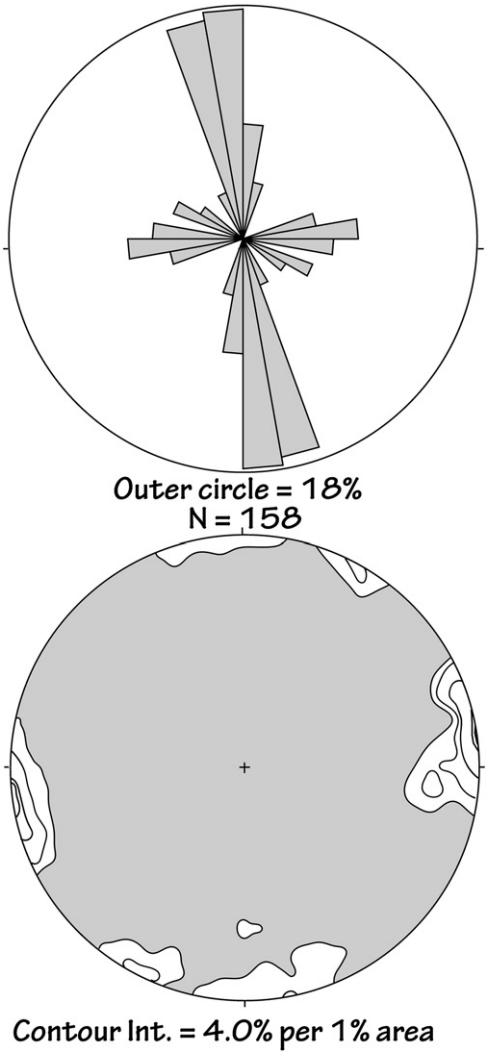

Fig. 5. Post-Permian joint set rose and density pole contour diagrams plotted in a Wulff stereonet. A main north–south set and two minor east–west and ~120° sets are shown. N is the number of measurements plotted.

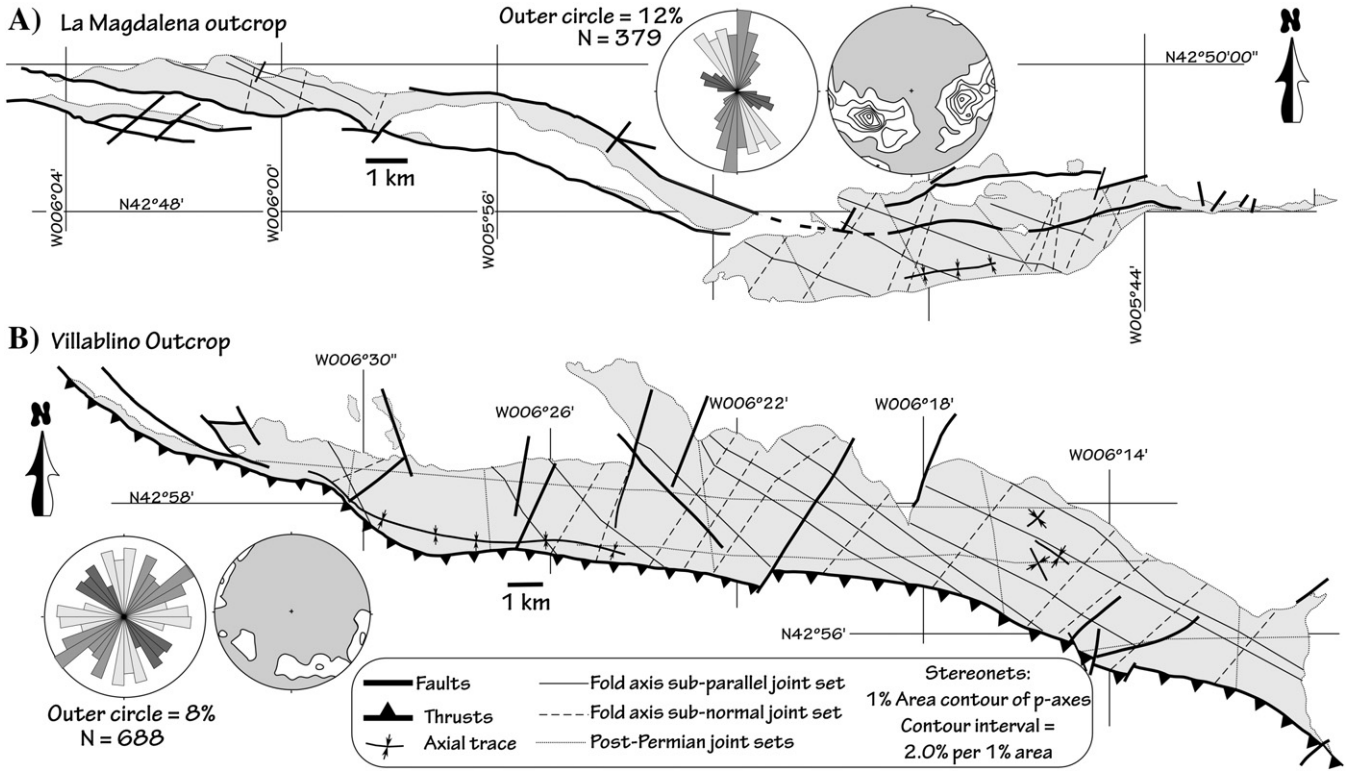

Fig. 6. A) Schematic sketch of the La Magdalena Stephanian outcrop plotting the trend of joint sets, rose and density pole diagrams. B) Schematic sketch of the Villablino Stephanian outcrop plotting the trend of joint sets, rose and density pole diagrams.

Van der Voo, 2002) using paleomagnetic declinations, but has recently been adopted by structural geologists to test various kinematic models of orogenic curvature using strain and fracture data (Yonkee and Weil, 2010a), calcite twin data (Kollmeier et al., 2000), and anisotropy of magnetic susceptibility lineations (Weil and Yonkee, 2009). In this paper, the trend of joint sets is compared to the regional structural trend in order to test different kinematic models for CAA development.

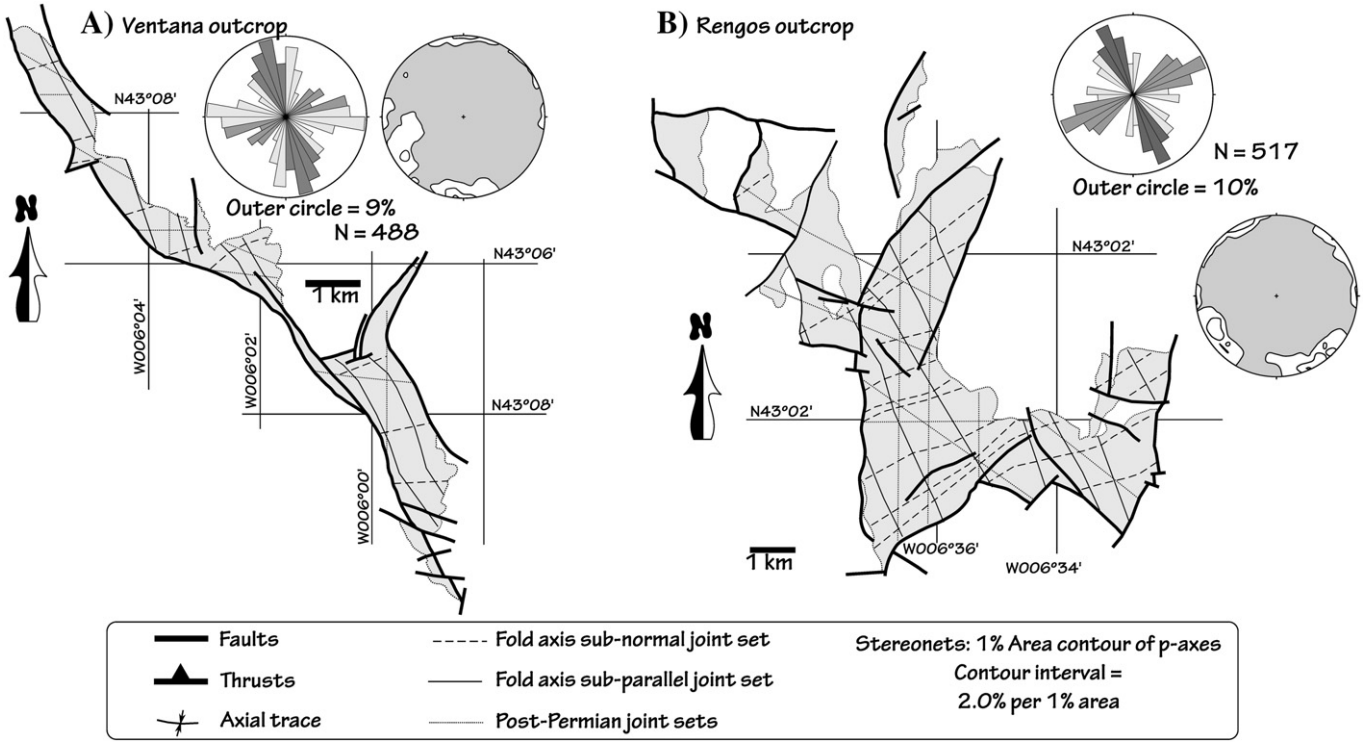

Fig. 7. Sketch of joint set orientations with their rose and pole density diagrams from Stephanian outcrops in the (A) Ventana and (B) Rengos.

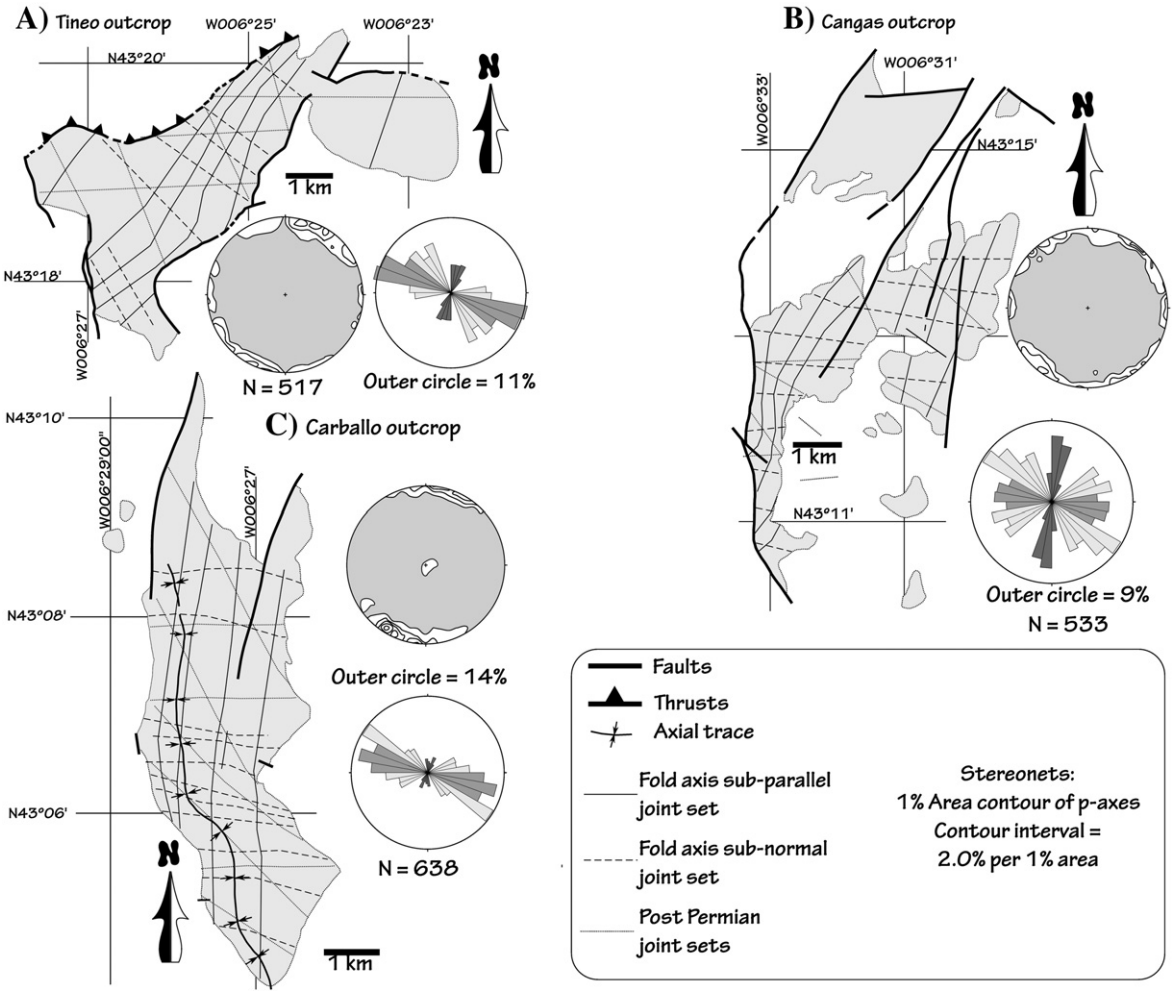

Fig. 8. Sketch of joint set orientations with their rose and pole density diagrams from Stephanian outcrops in the (A) Tineo, and (B) Cangas and (C) Carballo.

Fig. 2 shows simplified kinematic models for curved orogens using the orientation of systematic joint sets that are products of layer-parallel shortening fabrics. Model 2-A depicts a primary arc with no correlation between joint orientation and structural trend, which results in a strike tests with a slope of 0. Model 2-B is an alternative model for a primary arc with consistently oriented joint directions, however thrust slip is not uniform but radial, and thus the joint strike test yields a slope of 1.0. Model 2-C depicts a progressive arc with curved thrust slip, where joint orientations progressively rotate with structural trend resulting in a strike tests slope between 0 and 1.0 depending on the amount of curvature present when the joint sets develop. Model 2-D depicts an orocline (secondary bending of an originally linear belt), which yields a strike test slope of 1. However, since a joint strike test can produce a slope of 1.0 for primary arcs with radial slip and secondary oroclines, the strike test can only be uniquely interpreted if other kinematic constraints are available (Yonkee and Weil, 2010b).

Analysis of the different systematic joint sets present in the pre-, syn- and post-oroclinal rocks from the CAA supports kinematic and temporal interpretations made based on paleomagnetic data, and together indicate that the IAA is a secondary arc that was bent during uppermost Carboniferous (Stephanian) times.

2. Geological setting

The CAA includes the Cantabrian Zone (CZ) and the eastern part of the West Asturian–Leonese Zone (WALZ) (Fig. 3). The CZ is the foreland fold–thrust belt of the Western European Variscan Belt. Its sedimentary sequence consists of more than 7000 m of pre-orogenic Neoproterozoic arc-related and lower Paleozoic platform sediments that thin toward the core of the arc, and are covered by a Carboniferous syn-orogenic sequence. Deformation in the CZ is characterized by low finite strain values (Gutiérrez-Alonso, 1996; Pastor-Galán et al., 2009) and rocks do not show metamorphism except locally, where very low-grade metamorphic conditions are achieved (García-López et al., 2007; Gutiérrez-Alonso and Nieto, 1996). Permian magmatism is present in the CZ as small granite stocks, volcanic effusive rocks, dykes and sills (Valverde-Vaquero, 1992).

To the east and south of the CZ, the WALZ forms the internal zone, or hinterland, of the orogen and has intermediate to high strain rocks and greenschist facies metamorphism (i.e. Martinez and Rolet, 1988). The WALZ consists of more than 7000 m of Cambro-Ordovician sediments; the rest of the Paleozoic sequence is absent except for minor Silurian outcrops. In both zones the Paleozoic sequence unconformably overlies Upper Proterozoic slates and greywackes with minor intrusive, volcanic and volcanoclastic intercalations, which are more abundant toward the west (Fernandez-Suarez et al., 1998). The boundary between the WALZ and CZ consists of a major thrust and associated km-scale shear zone (Gutiérrez-Alonso, 1996).

Continental Stephanian B and C rocks (upper Kashimovian and Lower Gzhelian according to the new Carboniferous classifications of Gradstein et al., 2004) are widespread in the CZ and WALZ and unconformably overly the pre- and syn-orogenic sequences. The

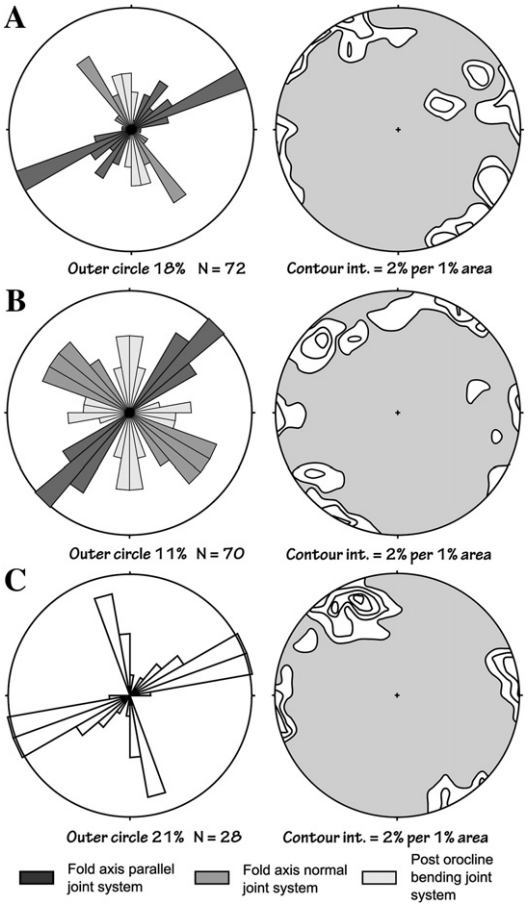

Fig. 9. Sketch of joint set orientations with their rose and pole density diagrams from Stephanian outcrops in the smaller (A) Arnao, (B) Buxeiro and (C) Combarcio outcrops.

Stephanian successions have little internal deformation and are well preserved and crop out in map-scale synforms that trend parallel to the trace of Variscan arc-parallel thrust faults (Alonso, 1989; Colmenero et al., 2008). The general structure of the Carboniferous synforms consists of a shallow dipping flank towards the core of the arc, and an outer steep to overturned flank. Contact of the Stephanian B and C rocks with the basement is, in some cases, a steep reverse fault (Fig. 3).

All Stephanian outcrops contain coal bearing continental sediments that show similar stratigraphic and sedimentological characteristics, and define a fining upwards sequence composed of breccias and polymodal conglomerates at the base, which are overlain by conglomerates with quartzitic pebbles interbedded with lithic sandstones, mudstones and coal seams, and capped by lithic sandstones, mudstones and coal seams (Colmenero and Prado, 1993; Corrales, 1971). The present distribution of Stephanian strata has been interpreted to reflect the original distribution of intermontane basins (Heward, 1978). Alternatively, given the similarity of their stratigraphic successions, it is also possible that the Stephanian succession was continuous across much of the western and southern portions of the CZ and WALZ (Corrales, 1971). In the core of the CAA there is a marine Stephanian sequence interpreted as the last remnants of a Gondwana passive margin in this sector of the Variscan belt (Merino-Tomé et al., 2009).

Early Permian mostly siliciclastic sedimentary and volcanic rocks of northern Iberia unconformably overlie rocks deformed during the Variscan, and thus post-date oroclinal bending of the IAA (Weil et al., 2010). The dominant lithologies are continental red conglomerates, red shales and sandstones, with minor limestones, volcanoclastic sediments and calc-alkaline basaltic lava flows with sparse isolated coal measures (Martínez-García, 1981; Suárez, 1988).

3. Results

3.1. General results

In order to document systematic joint sets in each of the three studied rock groups (pre-Stephanian, Stephanian and Permian outcrops), 172 measuring stations were analyzed in Stephanian outcrops (between 10 and 38 per outcrop), 64 stations in pre-Stephanian outcrops, and 6 stations in Permian outcrops. All studied rock units in

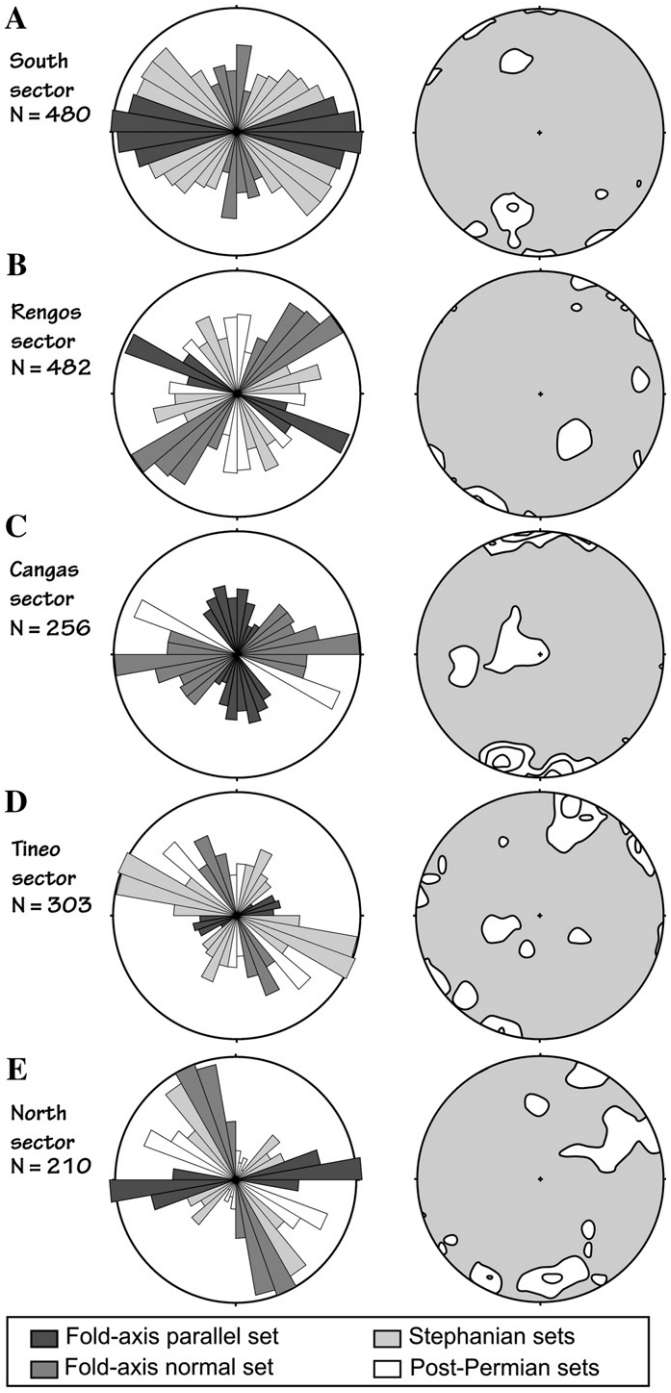

Fig. 10. Rose and pole density plots of the five sectors of pre-Stephanian rocks described in the text. They are ordered from South (A) to North (E).

the CZ and WALZ (Fig. 4) contain at least two systematic joint sets (Figs. 5–10). At least 30 joints per station were measured following the methodology described by Engelder and Geiser (1980).

All the joints recorded in Permian outcrops and the majority of joints observed in Stephanian outcrops depict characteristic plumose decoration of the joint planes when developed in fine grained clastic rocks, with no apparent record of shear (Fig. 11A). Lack of slip indicators suggests that the observed fractures originated as Mode I (tensile) cracks. Nevertheless, abundant joint surfaces in the pre-Stephanian outcrops do show evidence of shear re-activation that produced fibrous mineral lineations on joint surfaces with a sub-horizontal orientation, indicating a predominant strike-slip movement (Fig. 11B). For most of the observed fibrous lineations there was no criteria for establishing a shear-sense for joint reactivation. Nonetheless, in the few surfaces that did preserve well-defined kinematic criteria, dextral slip was dominant in the southern limb and sinistral slip was dominant in the northern limb of the CAA.

Intersecting and abutting relationships were carefully observed and documented in the field to establish the relative timing of the different joint sets. In the joint sets identified in the post-Permian rock sequences it was not possible to recognize enough abutting relationships to establish a temporal sequence for their development. It is noteworthy however, that when post-Permian joints are developed in pre-Permian rocks sequences they depict abutting relationships with existing joint sets, confirming their temporal sequence of development (Fig. 12A). In some cases post-Permian joints cross-cut existing joint sets, indicating that most of the joints were likely cemented and thus did not act as a free surface to arrest joint propagation.

In pre-Stephanian rock sequences abutting relationships are observed between those joint sets that are sub-parallel and sub-perpendicular to the regional trend, and those joint sets that are oblique to the present-day structural trend. In all cases where the two joint set families are distinguishable, the oblique sets abut against the sub-parallel and sub-perpendicular sets. This is particularly evident in the north and south limbs of the orocline, where the joint sets show the largest differences in azimuthal orientation. In the hinge zone (mainly in the Cangas sector), however, it is not possible to distinguish the two joint families (Fig. 13, Tables 2 and 3) as their similar orientations preclude their unique identification.

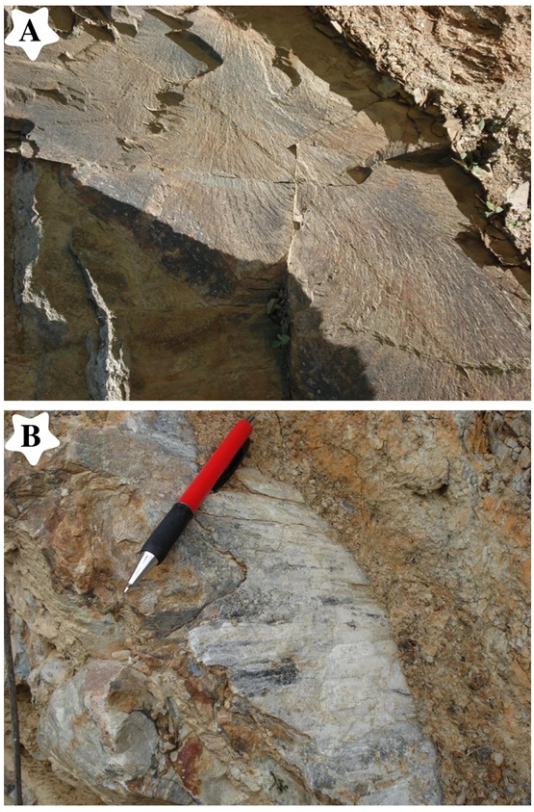

Fig. 11. A) Example of a plumose joint in Carballo outcrop preserved due to lack of reactivation. B) Picture of fibrous minerals produced by reactivation of joints as strike-slip faults in the Cangas sector.

Joint sets were categorized according to orientation criteria and abutting relationships. Bracketing unconformities were used to provide temporal control on the relative timing of the different joint sets. Joint sets present in the youngest rock sequence (i.e., above the bounding unconformities) are subtracted from those joint set populations measured in the oldest rock sequences (i.e., below the bounding unconformities). Thereby distinguishing those joint sets generated prior to the deposition of the overlying uncomfortable rocks.

All indentified joint sets depict sub-vertical dips making them comparable using rose diagrams. Only in outcrops from the southern branch of the CAA are there joint sets with dips of ca 65°–75° (interpreted to be slightly tilted by the effects of Mesozoic deformation in the area) (Alonso et al., 1996). Backtilting of the aforementioned joint sets was performed and the orientations obtained were statistically identical to their in situ orientations.

Three joint sets are distinguished in the Permian basins (Fig. 5; Table 1), each having a constant orientation. The most prominent set is oriented north–south with a strike of ~170°; secondary and tertiary sets are oriented east–west at ~90°, and northeast–southwest at ~130°. These joint sets have been described over the entire CAA in the pre-Permian rocks with little azimuthal variation with respect to regional trend (Table 1).

The joint sets present in Stephanian rocks have a more complicated pattern (Figs. 4–6; Tables 1 and 2). In addition to the uniform joint sets found in the overlying Permian rocks, all Stephanian outcrops have a joint set that is sub-parallel to local basin-scale fold axes ("strike set" or "strike-parallel joints" in Engelder and Geiser, 1980) and a second joint set that is sub-normal to these fold-axes. These sets exhibit a variation of less than ±10° within individual stations of the same outcrop (Table 2).

The outcrops studied from south to north are: the La Magdalena outcrop, which trends about east–west (Fig. 6A) and the Villablino outcrop, which has a trend of about 110° (Fig. 6B). Both outcrops are positioned in the southern limb of the CAA. The Ventana outcrop, which trends about 140° (Fig. 7A) and the Rengos outcrop, which has a regional strike of about 150° (Fig. 7B), are both situated in the southern limb of the CAA, but close to the arc hinge. The north–south trending, slightly curved, Cangas del Narcea (Fig. 8B) and Carballo (Fig. 8C) outcrops are located in the hinge of the arc, and the Tineo outcrop has a regional strike of about 30°, and is located slightly to the north of the Cangas del Narcea and Carballo localities (Fig. 8A).

Three additional smaller outcrops were studied but are not included in the tables — the northernmost Arnao (Figs. 2 and 8A), Buxeiro (Figs. 2 and 8B) and Combarcio (Figs. 2 and 8C) outcrops. Only one station in each outcrop provided date due to lack of sufficient exposure. The Arnao and Buxeiro regions have similar strike parallel (~60° and ~40° respectively) and strike sub-normal (~140° and ~130° respectively) joint sets; whereas, the Combarcio outcrop (Fig. 9C) had very limited exposure and did not yield enough data for interpretable results.

In the La Magdalena, Villablino, Cangas and Tineo outcrops, those joint sets that are indistinguishable from the post-Permian joint sets are not included in further analysis (marked with an asterisk in Table 1).

In order to compare the Stephanian outcrop joint sets with joint sets preserved in the underlying pre-Stephanian rocks, the pre-Stephanian outcrops are separated into five groups distributed along the trace of the CAA. The groups are arranged based on a consistent

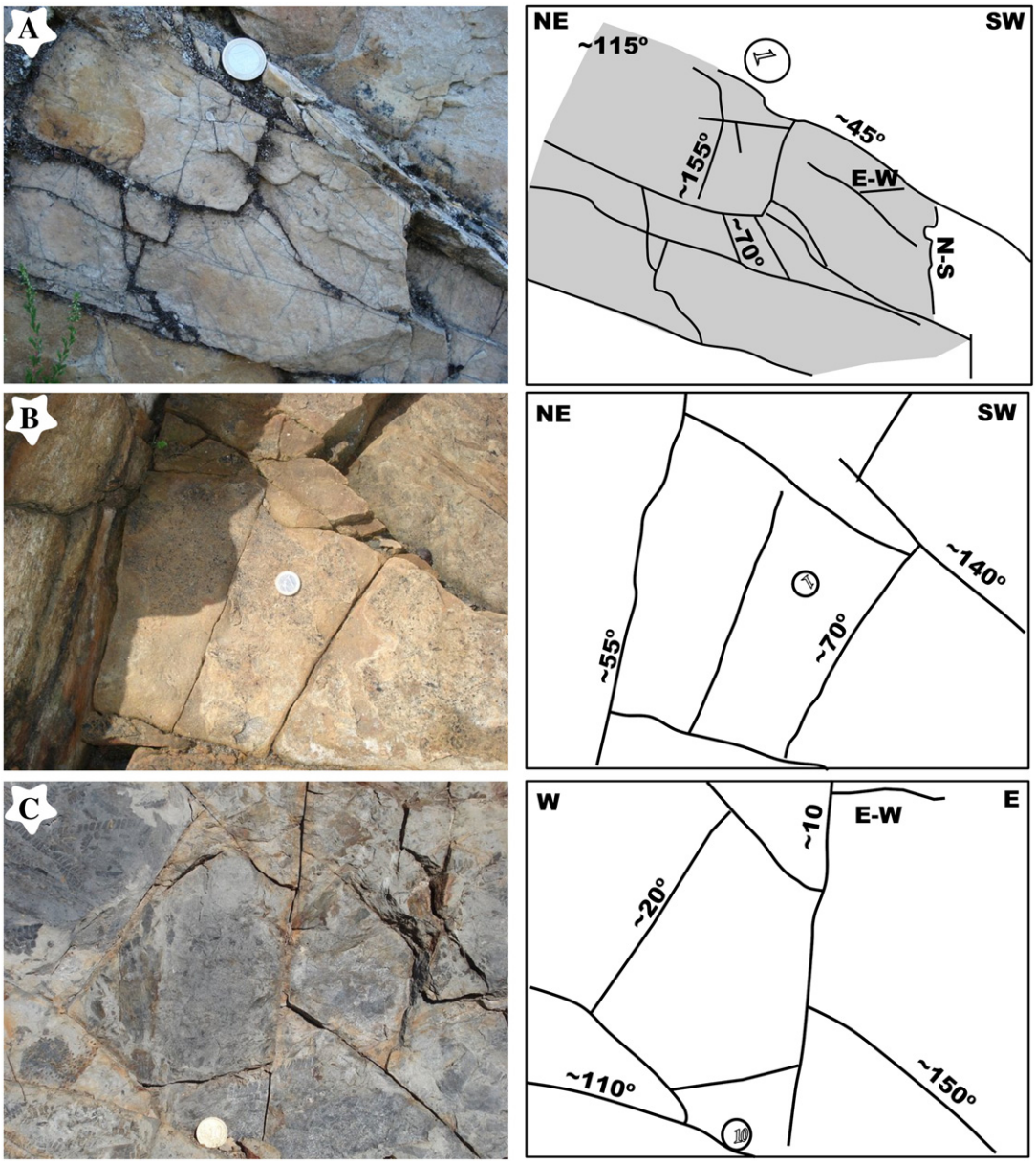

Fig. 12. Photographs depicting the intersecting and abutting relationships between joint sets in the pre-Stephanian and Stephanian rocks. A) Photograph and interpretation depicting the abutting relationships between pre-Stephanian, Stephanian and post-Permian joint sets. This photograph was taken in the Rengos sector near the Ventana outcrop. The gray shade represent a joint parallel to the photograph B) Photograph taken in the La Magdalena outcrop with a sketch of the interpreted joint sets showing their measured orientations. C) Photograph taken in Arnao outcrop with a sketch of the interpreted joint sets showing their measured orientations.

structural trend between outcrops (Fig. 3). Each group contains data from between 10 and 15 outcrops. Each of the five pre-Stephanian groups corresponds with at least one studied Stephanian outcrop for comparison. The five groups are: (i) the southern sector, which underlies the La Magdalena, Villablino and part of the Ventana outcrops (Fig. 9A); (ii) the Rengos sector, which covers the Rengos, Ventana and southern limit of the Carballo outcrops (Fig. 9B); (iii) the Cangas del Narcea sector, which extends around the Cangas del Narcea and northern portion of the Carballo outcrops (Fig. 9C); (iv) the Tineo sector, which contains the Tineo, Buxeiro and Combarcio outcrops (Fig. 10D); and (v) the north sector, which covers all the pre-Stephanian outcrops north of the Tineo outcrop (Fig. 10E).

Both the Permian and Stephanian joint sets have been described in these zones. In addition longitudinal fold-axis parallel and fold-axis normal joint sets are observed (Table 3) and, because of their orientation relative to the folds, are interpreted to be tensile fractures (Hancock, 1985). As observed in Stephanian outcrops, some of the post-Permian and Stephanian joint sets are coincident with the pre-Stephanian sets and are thus tagged with an asterisk in Tables 1 and 2.

The orientations of the examined joint sets are summarized in Fig. 14, where the general trends of pre-Stephanian (A), Stephanian (B) and post-Permian (C) joint sets are traced across the present-day CAA. It is noteworthy that the joint sets that were only found in the pre-Stephanian outcrops have a dramatic spatial change in orientation that mimics the present structural trend of the CAA, while those joint sets found in younger Stephanian outcrops have a spatial change in orientation that has a more subtle curved trace. Finally, the joint sets described from Permian outcrops have no significant change in their spatial orientation.

3.2. Strike test

Strike tests have been performed on each of the three joint set categories: those found in (i) the pre-Stephanian, (ii) Stephanian and

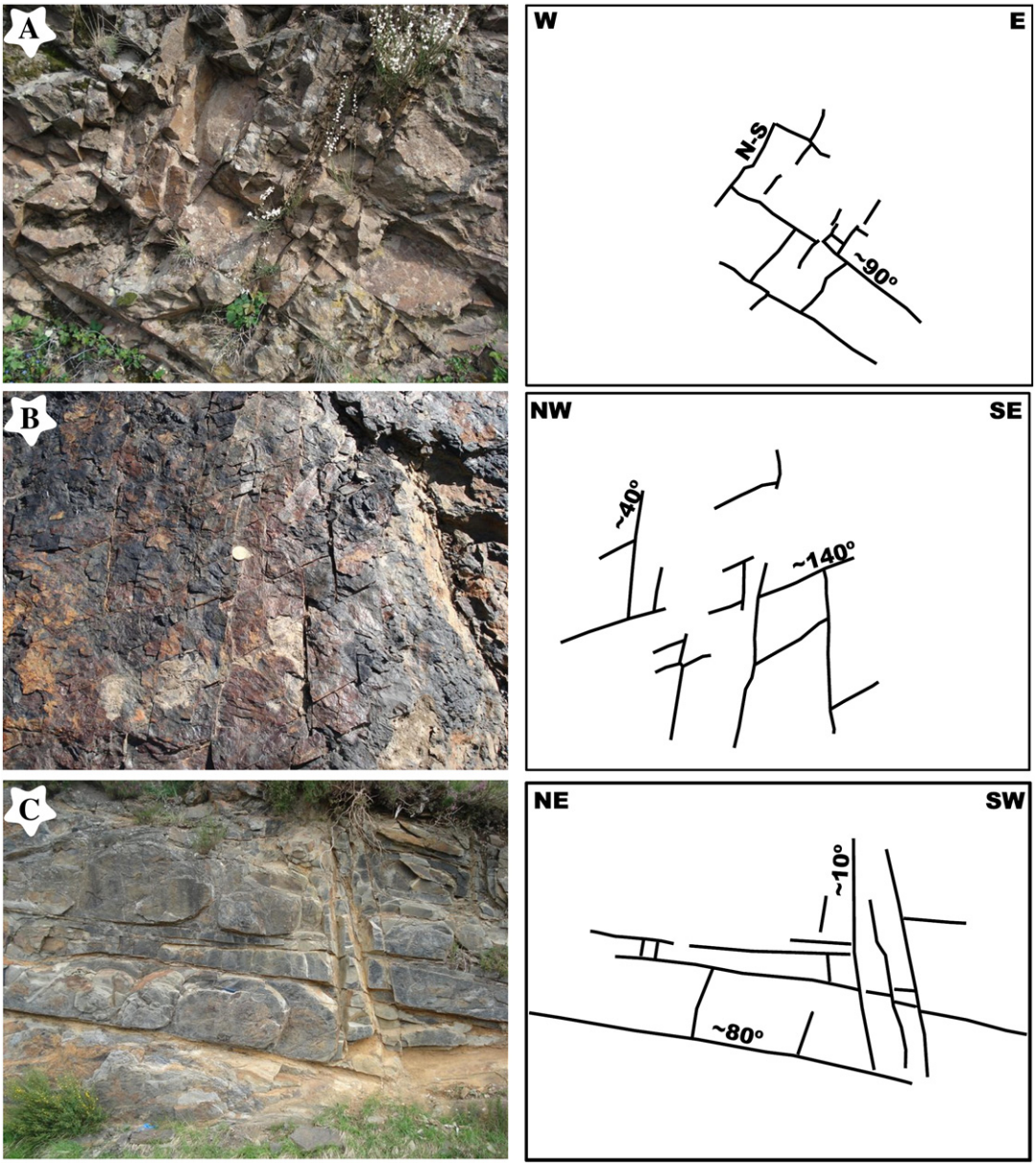

Fig. 13. Photographs depicting the intersecting and abutting relationships between the strike sub-parallel and sub-normal sets in the Stephanian rocks. The joint sets that abut each other are interpreted to have developed coevally. A) Photograph and interpreting sketch depicting the joint abutting relationships in Cangas outcrop. B) Photograph taken in the Villablino outcrop with a sketch of the interpreted joint sets showing their measured orientations. C) Photograph and sketch of the interpreted joint sets taken in Carballo outcrop.

(iii) Permian outcrops. All strike tests were done using the refined weighted least-squares method of Yonkee and Weil (2010b).

Strike tests for all three Permian outcrop joint sets (Fig. 14) give a slope of near 0.0 ($-0.03 \pm .08$, $0.09 \pm .08$, $0.00 \pm .08$), implying that the joint sets in these rocks show to significant correlation with changes in structural trend around the CAA.

Fig. 16 shows strike tests for the Stephanian outcrop joint sets. Mean structural trend of Variscan structures below the Stephanian outcrop were used as reference trend values for the individual sites. Strike tests were done with the Stephanian outcrop strike sub-parallel (Fig. 16A) and sub-normal joint sets (Fig. 16B). Slopes of $0.72 \pm .18$ and $0.57 \pm .12$ are calculated for the two sets respectively.

The fold-axis parallel joint set (14-A) and fold-axis normal joint set (14-B) from the pre-Stephanian outcrops (Fig. 17) have strike test slopes close to 1.0 ($1.03 \pm .06$ and $1.16 \pm .10$ respectively). These results indicate a significant one-to-one correlation between deviations in structural trend and joint set orientation, and suggest that the joint sets pre-date any vertical-axis rotations and that the total deviation in trend of pre-Stephanian outcrop joint sets is about a third greater than that found in the Stephanian outcrop joint sets.

4. Discussion

Results from joint set analysis in the three unconformity bounded sedimentary sequences from the CAA reveal the existence of at least three different deformation episodes in which joints developed. Regional joint sets are classically interpreted as from the result of far-field tectonic stresses (e.g., Engelder and Geiser, 1980; Eyal et al., 2001; Gross et al., 1995). When used together with other structures, like folds and faults, these joint sets can be extremely valuable in unraveling the geological stress–strain history of a region (e.g., Engelder and Geiser, 1980; Engelder and Gross, 1993). In general, joints develop within the σ_1–σ_2 plane, which in previously undeformed contractional settings is roughly normal to the axis of the folds

Table 1
Post-Permian joint sets in every outcrop studied. Mean strike showing a confidence interval with a confidence level of 95% ($\alpha = 0.05$). Joint-sets labeled with * were indistinguishable from the Stephanian joint sets and those joint sets labeled with ** were indistinguishable from the pre-Stephanian ones, thus they were analyzed together (full explanation in text).

Post Permian joint sets	Stations	Set 1 (N–S)		Set 2 (E–W)		Set 3 (~130)	
		Mean strike	Standard deviation	Mean strike	Standard deviation	Mean strike	Standard deviation
Permian outcrops							
	6	174° ± 2	10°	86° ± 3	11°	123° ± 3	6°
Stephanian outcrops							
La Magdalena	13	10° ± 2*	13°	111° ± 3*	14°	149° ± 1	7°
Villablino	22	176° ± 2	10°	92° ± 2	13	141° ± 2*	10°
Rengos	23	183° ± 2	10°	90° ± 1	8°	128° ± 2	8°
Ventana	18	188° ± 2	10°	92° ± 2	8°	126° ± 2	7°
Carballo	38	175° ± 1	5°	83 ± 1	9°	131 ± 2	12°
Cangas	26	5° ± 2*	9°	83 ± 2	13°	133 ± 2	11°
Tineo	23	14° ± 2*	10°	95° ± 2	11°	149° ± 1	8°
Pre-Stephanian outcrops							
South sector	13	176° ± 3**	13°	90° ± 2**	15°	134° ± 2*	12°
Rengos sector	15	183° ± 2	10°	87° ± 2	6°	115°2**	9°
Cangas–Carballo sector	12	170° ± 5*	19°	80° ± 3*	20°	120° ± 3	8°
Tineo sector	12	181° ± 1	7°	108° ± 2*	9°	139° ± 1	5°
North sector	12	177° ± 4	8°	88° ± 3**	9°	125° ± 3	7°

that accommodate shortening (Engelder and Geiser, 1980; Whitaker and Engelder, 2006).

The different orientations of joint sets found in the CAA help to unravel the timing and kinematic history of arc formation. Based on abutting relationships the youngest joint sets generated in the studied region are recorded in the Permian outcrops (Figs. 4 and 14C). The north–south set, and likely the east–west set, are interpreted to be caused by bedding flexure during Alpine northward collision of Iberia with Western Europe in Cenozoic times (e.g., Alonso et al., 1996; Álvaro et al., 1979). Based on their regional tectonic orientations, the third joint set, which strikes ~130°, is interpreted to be caused by the Betic orogen during Alpine northwestward collision between Africa and Europe. These interpretations are mainly based on the correlation of joint set orientations with the trend of major structures in post-Carboniferous rocks as well as previously published regional paleostress orientations (e.g., Andeweg, 2002; Cloetingh et al., 2002). Because deposition of the Permian strata is known to have post-dated deformation associated with the formation of the IAA (Weil et al., 2010), these joints have been removed from consideration in the analyses of older rock joint sets.

The Stephanian outcrops record two joint sets that are not found in post-Stephanian Permian outcrops (Fig. 10B). The longitudinal set has an arcuate pattern with lower overall curvature than the trends of the underlying structures (Fig. 15A). The orthogonal set shows a radial pattern, sub-perpendicular to the main underlying Variscan structural trend (Fig. 15B). Field relations suggest that the two sets usually abut each other, which is interpreted to represent their coeval formation (Fig. 12) related to the regional stress field proposed by Caputo (1995, 2010) and Bai et al. (2002).

The pre-Stephanian (Neoproterozoic and Paleozoic) outcrops record a complex set of joint sets that include all the Stephanian and younger joint sets as well as at least two older sets that are sub-parallel and sub-perpendicular to the main Variscan structural trend. One of the sets is parallel to the main Variscan structural grain (e.g., fold axis and thrust trends), which mimics the trace of the CAA, and the other set is perpendicular to the arc (Fig. 15).

To explain the temporal and spatial distribution of joint sets in the region we have assigned each unconformity-bound joint set to a stress field responsible for their generation. The appropriate tectonic stress field(s) responsible for the joint sets present in the Stephanian and pre-Stephanian outcrops is less straight forward to assign. Given the significant correlation between joint orientation and the arcuate trace of the CAA, it is difficult to imagine a process that could have formed in situ joint sets with a primary dispersion of 180° for the pre-Stephanian outcrop sets (strike tests slopes of near unity), and joint sets with between 90° and 125° of primary dispersion for Stephanian

Table 2
Stephanian joint sets in every outcrop studied. Mean strike showing a confidence interval with a confidence level of 95% ($\alpha = 0.05$). Joint-sets labeled with * were indistinguishable from the pre-Stephanian joint sets therefore they were analyzed together (full explanation in text).

Stephanian joint sets	Stations	Sub-parallel set		Sub-perpendicular set	
		Mean strike	Standard deviation	Mean strike	Standard deviation
Stephanian outcrops					
La Magdalena	13	111° ± 3	14°	10° ± 2	13°
Villablino	22	141° ± 2	10°	50° ± 2	12°
Rengos	23	154° ± 2	7°	60° ± 1	7°
Ventana	18	154° ± 2	9°	59° ± 2	12°
Carballo	38	14° ± 3	9°	105° ± 1	6°
Cangas	26	5° ± 2	9°	105° ± 1	11°
Tineo	23	14° ± 2	10°	124° ± 1	7°
Pre-Stephanian outcrops					
South sector	13	134° ± 2	12°	46° ± 3	12°
Rengos sector	15	154° ± 2	8°	68° ± 2	11°
Cangas–Carballo sector	12	170° ± 5*	19°	80° ± 3*	20°
Tineo sector	12	29° ± 2	7°	108° ± 2	9°
North sector	12	49° ± 3	8°	142° ± 2	6°

Table 3
Pre-Stephanian joint sets in every outcrop studied. Mean strike showing a confidence interval with a confidence level of 95% ($\alpha = 0.05$).

Pre-Stephanian joint sets	Stations	Parallel set		Perpendicular set	
		Mean strike	Standard deviation	Mean strike	Standard deviation
Pre-Stephanian outcrops					
South sector	13	90° ± 2	15°	176° ± 3	13°
Rengos sector	15	115° ± 2	9°	45° ± 2	9°
Cangas–Carballo sector	12	170° ± 5	19°	80° ± 3	20°
Tineo sector	12	73° ± 2	7°	153° ± 2	9°
North sector	12	88° ± 3	9°	160 ± 2	4°

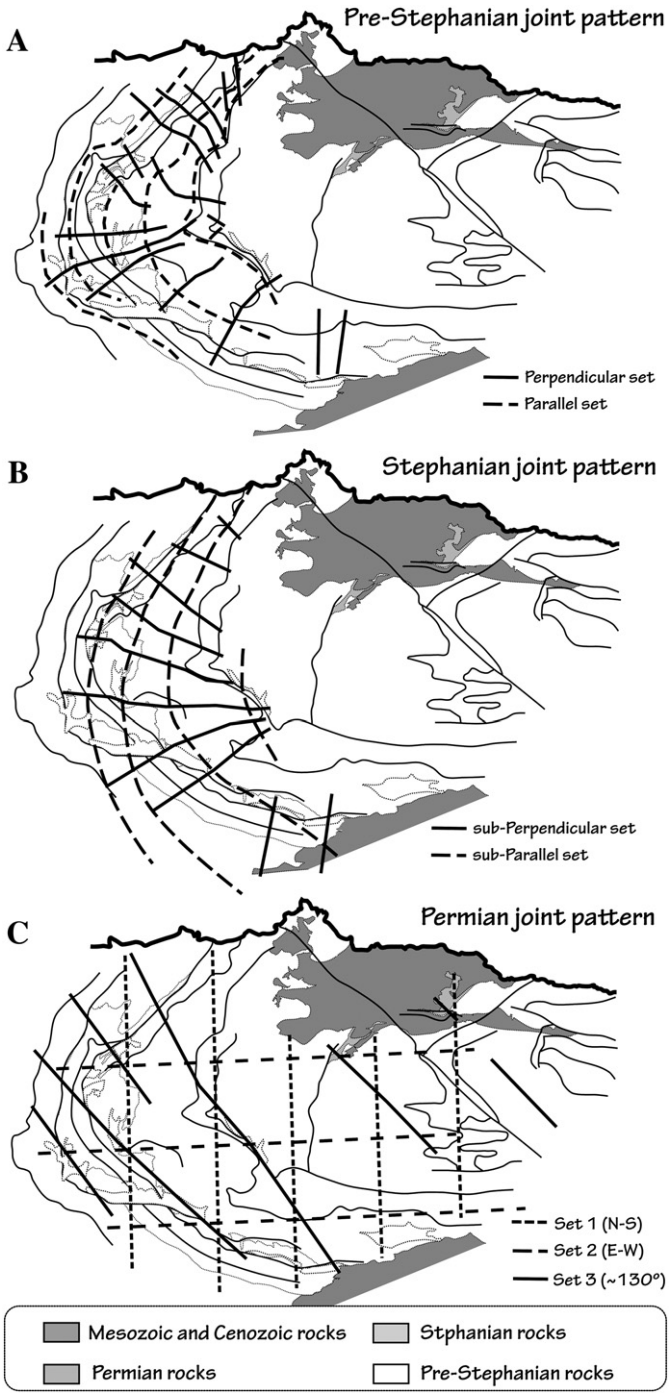

Fig. 14. Schematic sketch showing the envelope of joint azimuths traced for the (A) pre-Stephanian joint-pattern, (B) Stephanian joint-pattern, and (C) post-Permian joint-patterns found in the CAA.

outcrops (based on strike test slopes of between 0.5 and 0.7). Given the existing paleomagnetic data that indicate large-scale rotation of Variscan structures during Stephanian and younger times (e.g., Van der Voo et al., 1997; Weil et al., 2000, 2001), it is more conceivable that the joint sets were formed with a regionally linear north–south trend (in present-day coordinates) and were subsequently rotated to their present orientation. Consequently, the pre-Stephanian and Stephanian outcrops record joint sets formed prior to, and penecontemporaneous with, oroclinal bending. Thus, the present orientation of joint sets in pre-Stephanian outcrops are the result of ca. 180° of vertical-axis rotation of an approximately linear joint set that was parallel to early longitudinal fold axes; while the Stephanian outcrop joint sets show a rotation of ca. 100°, undergoing between 50 and 70% of the total oroclinal rotation.

The simplest tectonic scenario that explains these observations indicates that two linear sets of joints formed coevally with the main Variscan shortening in the western part of the CZ during the uppermost Mississippian–early Pennsylvanian. Subsequently, these sets were rotated ca. 90° around vertical-axes prior to deposition of

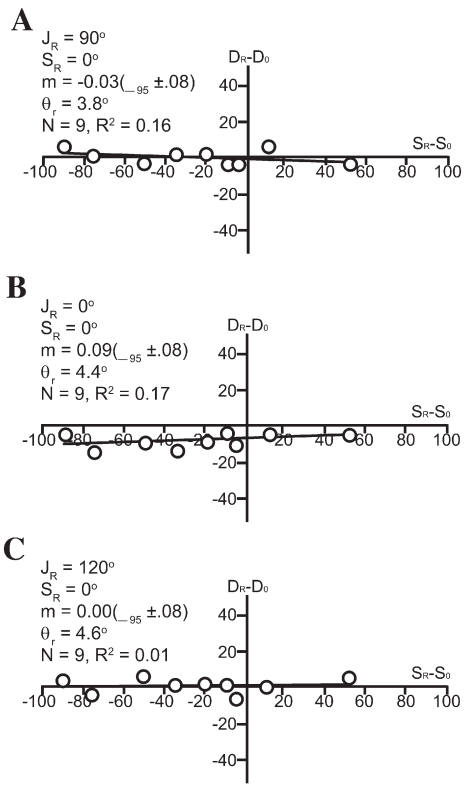

Fig. 15. Strike test plots of the post-Permian joint sets. A) Plot of east–west joint set, B) plot of the north–south joint set and C) plot of the ~120° joint set. Least-square regressions of the three data sets have slopes of close to 0, indicating that the CAA was completely closed at Permian times. Reference joint strike (J_R) and reference strike (S_R) best-fit slopes (m), 95% confidence intervals (in parentheses), number of sites (N), and standard deviation of the residuals (θ_R) are listed.

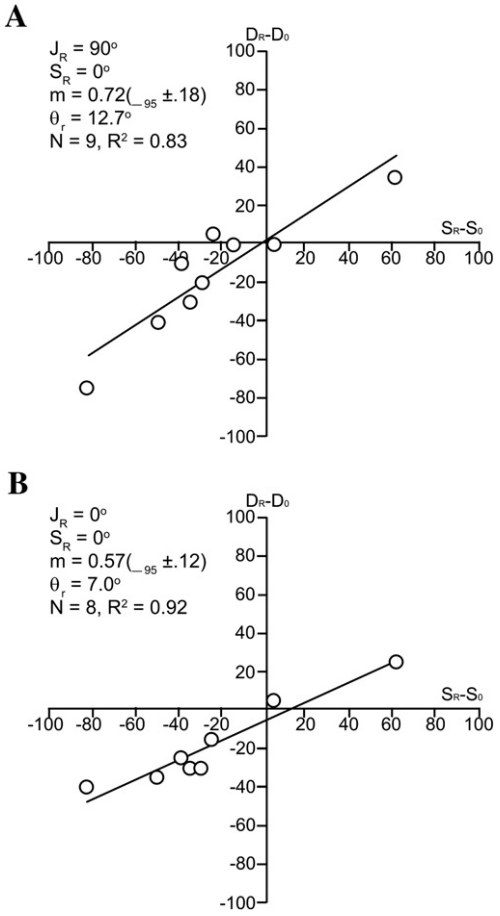

Fig. 16. Strike test plots of the Stephanian joint sets. A) Strike sub-parallel sets have a slope of 0.72 and B) strike sub-normal sets have a slope of 0.51. Reference joint strike (J_R) and reference strike (S_R), best-fit slopes (m), 95% confidence intervals (in parentheses), number of sites (N), and standard deviation of the residuals (θ_R) are listed.

Stephanian sediments. Finally, the arc was tightened another ca. 90° to its present-day curvature between the Stephanian and earliest Permian.

Joints formed during the east–west shortening stage that gave rise to the Cantabrian fold–thrust belt likely accommodated some of the vertical axis rotation, as evidenced by their reactivation. However, it was the larger structural anisotropies (e.g., thrusts and vertical strike-slip faults) that likely absorbed most of the strain associated with rotations (Alonso et al., 2009; Gutiérrez-Alonso et al., 2004).

The joint data analyzed herein is interpreted in light of the previously proposed CAA oroclinal bending model (e.g. Gutiérrez-Alonso et al., 2004, 2008; Stewart, 1995; Weil, 2006; Weil et al., 2001, 2010). This model requires an initial east–west (in present-day coordinates) compression event that produces a near-linear orogen. This compression is followed by a sudden change to north–south shortening (in present-day coordinates) that rotates the limbs of the orogen and is recorded in the latest thrusts of the Cantabrian Zone (Merino-Tomé et al., 2009). This model suggested a brief period of time (around 15 Ma) for oroclinal bending, from the latest Carboniferous to the earliest Permian. Time constraints are based on assigned magnetization ages for rocks sampled in the CZ, importantly the post-arc-parallel folding but pre-orocline paleomagnetic B component that was interpreted as late Carboniferous to early Permian in age (Van der Voo et al., 1997; Weil et al., 2000; 2001). This magnetization has been reinterpreted as Kasimovian in age based on estimated timing of arc-parallel folding inferred from syntectonic sediments. Upper age bounds are given by the eP magnetization found in Permian basins from the northern and southern arms of the larger Ibero-Armorican Arc, thus constraining oroclinal bending to a 10 Ma time interval (see Weil et al., 2010). The relative age of progressive joint set formation in the CAA, as constrained by the ages of the bounding unconformities, agrees well with the existing paleomagnetic constraints for oroclinal bending of the CAA.

According to results from the joint set strike tests, prior to Stephanian B–C times the CAA was closed between 30% and 50%, and by lower-most Permian times was completely closed. Assuming a constant bending rate, about 100° of bending took 5 Ma from Stephanian B–C (upper-most Kasimovian ~304 Ma) to the Carboniferous–Permian limit (299 Ma). Consequently, the remaining curvature of the CAA had to be produced before the generation of the joints in the Stephanian rocks and, if the bending rate was similar to that of Stephanian times, it is likely that the CAA started bending during the Moscovian (around 310 Ma). This chronology reinforces the interpretation of the rapid tectonic lithospheric delamination event proposed by Gutiérrez-Alonso et al. (2004, 2011) (Fig. 17).

To better illustrate the kinematics model of fracture set evolution, we present an animation (Video 1 which can be downloaded from the Data Repository with higher resolution; summarized in Fig. 18). Fig. 18A represents the pre-Moscovian to Moscovian pre-oroclinal bending times with the fold-axis parallel and normal joint sets recorded in pre-Stephanian outcrops. Fig. 18B represents lower Kasimovian times with the Leon breaching thrust already formed (Alonso et al., 2009) and approximately 20% bending. Fig. 18C shows initial southward emplacement of the Picos de Europa and Cuera units

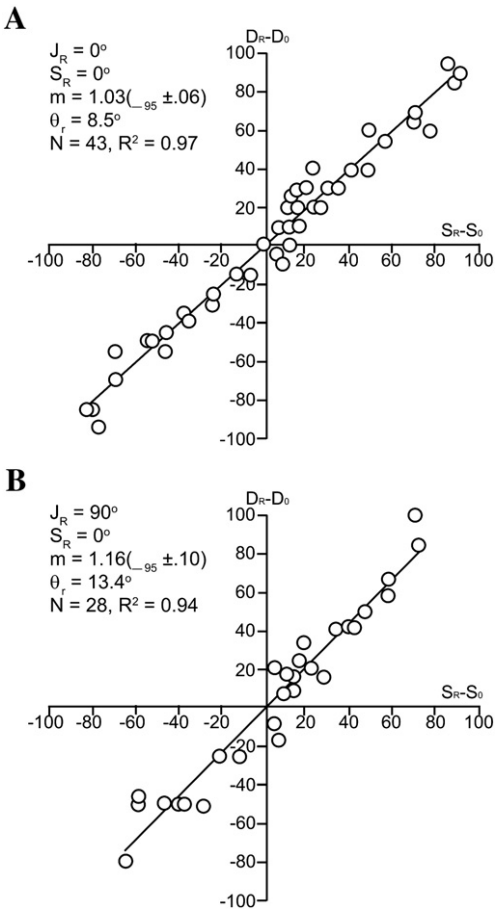

Fig. 17. Strike test plots of the pre-Stephanian joint sets. A) Strike parallel sets have a slope of 0.96 and B) strike sub-normal sets have a slope of −1.03. Reference joint strike (J_R) and reference strike (S_R), best-fit slopes (m), 95% confidence intervals (in parentheses), number of sites (N), and standard deviation of the residuals (θ_R) are listed.

(Merino-Tomé et al., 2009), deposition of the Stephanian B–C sediments, development of fold-axis sub-parallel and sub-perpendicular joint sets recorded in Stephanian outcrops, and 50–70% bending. Fig. 18D represents the final present-day stage with the addition of post-Permian aged joints imprinted across the entire CAA.

5. Conclusions

The study of systematic joint sets in rock sequences bounded by unconformities, allows for potentially robust timing constraints on joint formation, and can provide geometric constraints on changes in the regional stress field. Such constraints can help unravel the kinematics of regions where other structural criteria are unavailable.

Joint pattern analysis in the CAA reveals the presence of at least three different phases of joint development: (i) during east–west (in present-day coordinates) compression related to the collision between Gondwana and Laurentia and the development of the Variscan foreland fold–thrust belt; (ii) during north–south compression that resulted in oroclinal bending of the CAA, and (iii) during post-Permian times. Joint patterns in the CAA indicate that the CAA was closed between 30% and 50% prior to Stephanian times, and was completely bent by the lowermost Permian. These kinematic constraints, together with previous data, indicate that oroclinal bending of the CAA occurred from middle Moskovian to the Carboniferous–Permian boundary (between 310 and 299 Ma). The results of this study support the secondary nature of the Ibero-Armorican Arc.

Supplementary materials related to this article can be found online at doi:10.1016/j.tecto.2011.05.005.

Acknowledgments

This paper is part of the IGCP Project from UNESCO No. 574: Bending and Bent Orogens, and Continental Ribbons. Financial support was supplied by Research Projects ODRE and ODRE II ("Oroclines and Delamination: Relations and Effects") No. CGL2006-00902 and

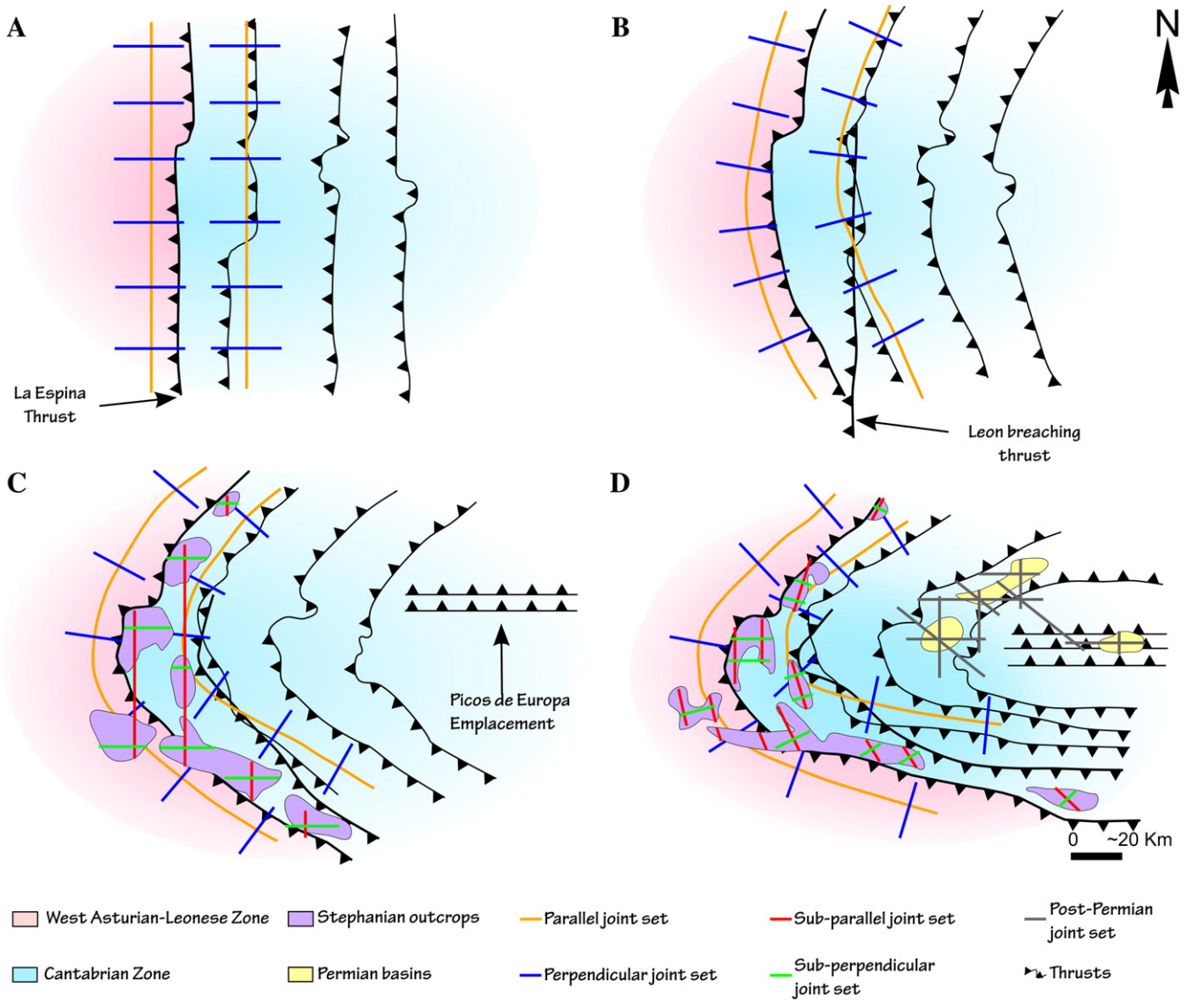

Fig. 18. Cartoon summarizing the animation presented in the included data repository. Schematic plates depict the development of joint sets in the Cantabrian and West-Asturian Leonese zones of the CAA during formation of the Ibero-Armorican orocline. A) Shows the joints interpreted to develop contemporaneous with formation of a nearly linear Variscan orogen in pre-Moscovian and Moscovian times. B) Shows the first phase of orocline development during Kasimovian times, with the Leon breaching thrust already formed (Alonso et al., 2009) and around 20% of present-day curvature already attained. C) Depicts the CAA during the uppermost Kasimovian and Gzhelian times when between 30 to 50% of the arc's present-day curvature was attained, initial emplacement of the Picos de Europa and Cuera units occurred, deposition of the Stephanian B–C basins occurred, and development of fold-axis sub-parallel and sub-perpendicular Stephanian joint sets were formed. D) Shows the final present-day geometry of the CAA.

CGL2009-1367, from the Spanish Ministry of Science and Innovation. DPG is also granted by an ACPI grant from the Junta de Castilla and Leon. Thanks also to F. Storti, S. Marshak and R. Caputo for his helpful, critical and constructive review of the manuscript.

References

Aller, J., Gallastegui, J., 1995. Analysis of kilometric-scale superposed folding in the central coal basin (Cantabrian zone, NW Spain). Journal of Structural Geology 17 (7), 961–969.

Alonso, J.L., 1989. Fold reactivation involving angular unconformable sequences — theoretical-analysis and natural examples from the Cantabrian zone (northwest Spain). Tectonophysics 170 (1–2), 57–77.

Alonso, J.L., Pulgar, J.A., García-Ramos, J.C., Barba, P., 1996. Tertiary basins and Alpine tectonics in the Cantabrian Mountains (NW Spain). In: Friend, P.F., Dabrio, Cristino J. (Eds.), Tertiary Basins of Spain, World and Regional Geology. Cambridge University Press, Cambridge.

Alonso, J.L., Marcos, A., Suarez, A., 2009. Paleogeographic inversion resulting from large out of sequence breaching thrusts: the Leon Fault (Cantabrian Zone, NW Iberia). A new picture of the external Variscan Thrust Belt in the Ibero-Armorican Arc. Geologica Acta 7 (4), 451–473.

Alvarez-Marron, J., Perez-Estaun, A., 1988. Thin skinned tectonics in the Ponga region (Cantabrian Zone, NW Spain). Geologische Rundschau 77 (2), 539–550.

Álvaro, M., Capote, R., Vegas, R., 1979. Un modelo de evolución geotectónica para la cadena celtibérica. Acta Geologica Hispanica 14, 172–177.

Andeweg, B., 2002. Cenozoic tectonic evolution of the Iberian Peninsula: causes and effects of changing stress fields. Ph. D. Thesis. VU University Amsterdam.

Bai, T., Maerten, L., Gross, M.R., Aydin, A., 2002. Orthogonal cross joints: do they imply a regional stress rotation. Journal of Structural Geology 24 (1), 77–88.

Brun, J.P., Burg, J.P., 1982. Combined thrusting and wrenching in the Ibero-Armorican arc — a corner effect during continental collision. Earth and Planetary Science Letters 61 (2), 319–332.

Caputo, R., 1995. Evolution of orthogonal sets of coeval extension joints. Terra Nova 7, 479–490.

Caputo, R., 2010. Why joints are more abundant than faults. A conceptual model to estimate their ratio in layered carbonate rocks. Journal of Structural Geology 32, 1257–1270.

Carey, S.W., 1955. The orocline concept in geotectonics. Royal Society of Tasmania Proceedings 89, 255–288.

Cloetingh, S., Burov, E., Beekman, F., Andeweg, B., Andriessen, P.A.M., García-Castellanos, D., De Vicente, G., Vegas, R., 2002. Lithospheric folding in Iberia. Tectonics 21, 1041–1067.

Colmenero, J., Suarezruiz, I., Fernandezsuarez, J., Barba, P., Llorens, T., 2008. Genesis and rank distribution of Upper Carboniferous coal basins in the Cantabrian Mountains, Northern Spain. International Journal of Coal Geology 76 (3), 187–204.

Colmenero, J.R., Prado, J.G., 1993. Coal basins in the Cantabrian Mountains, Northwestern Spain. International Journal of Coal Geology 23 (1–4), 215–229.

Corrales, I., 1971. La sedimentación durante el Estefaniense B–C en Cangas de Narcea, Rengos y Villablino (NW de España). Trabajos de Geología 3, 69–73.

Dunne, W.M., North, C.P., 1990. Orthogonal fracture systems at the limits of thrusting: an example from southwestern Wales. Journal of Structural Geology 12 (2), 207–215.

Eldredge, S., Bachtadse, V., Van Der Voo, R., 1985. Paleomagnetism and the orocline hypothesis. Tectonophysics 119 (1–4), 153–179.

Engelder, T., Geiser, P., 1980. On the use of regional joint sets as trajectories of paleostress fields during the development of the Appalachian plateau, New York. Journal of Geophysical Research 85, 6319–6341.

Engelder, T., Gross, M.R., 1993. Curving cross joints and the lithospheric stress field in eastern North America. Geology 21 (9), 817–820.

Eyal, Y., Gross, M.R., Engelder, T., Becker, A., 2001. Joint development during fluctuation of the regional stress field in southern Israel. Journal of Structural Geology 23 (2–3), 279–296.

Fernandez-Suarez, J., Gutierrez-Alonso, G., Jenner, G.A., Jackson, S.E., Fernandez-Suarez, J., Gutierrez-Alonso, G., Jenner, G.A., Jackson, S.E., 1998. Geochronology and geochemistry of the Pola de Allande granitoids (northern Spain): their bearing on the Cadomian–Avalonian evolution of northwest Iberia. Canadian Journal of Earth Sciences 35 (12), 1439–1453.

Fischer, M.P., Jackson, P.B., 1999. Stratigraphic controls on eformation patterns in fault-related folds: a detachment fold example from the Sierra Madre Oriental, northeast Mexico. Journal of Structural Geology 21 (6), 613–633.

García-López, S., Brime, C., Valín, M.L., Sanz-López, J., Bastida, F., Aller, J., Blanco-Ferrera, S., 2007. Tectonothermal evolution of a foreland fold and thrust belt: the Cantabrian Zone (Iberian Variscan belt, NW Spain). Terra Nova 19 (6), 469–475.

Gradstein, F.M., Ogg, J.G., Smith, A.G., 2004. A Geologic Time Scale 2004. Cambridge University Press, Cambridge.

Gross, M.R., Fischer, M.P., Engelder, T., Greenfield, R.J., 1995. Factors controlling joint spacing in interbedded sedimentary rocks: integrating numerical models with field observations from the Monterey Formation, USA. Geological Society, London, Special Publications 92 (1), 215–233.

Gutiérrez-Alonso, G., Nieto, F., 1996. White-mica 'crystallinity', finite strain and cleavage development across a large Variscan structure. NW Spain: Journal of the Geological Society 153, 287–299.

Gutiérrez-Alonso, G., 1996. Strain partitioning in the footwall of the Somiedo Nappe: structural evolution of the Narcea Tectonic window. NW Spain: Journal of Structural Geology 18 (10), 1217–1229.

Gutiérrez-Alonso, G., Fernandez-Suarez, J., Weil, A.B., Murphy, J.B., Nance, R.D., Corfu, F., Johnston, S.T., 2008. Self-subduction of the Pangaean global plate. Nature Geoscience 1 (8), 549–553.

Gutiérrez-Alonso, G., Fernández-Suárez, J., Weil, A.B., 2004. Orocline triggered lithospheric delamination. In: Weil, A.B., Sussman, A. (Eds.), Special Paper. Geological Society of America, Boulder, pp. 121–131.

Gutiérrez-Alonso, G., Murphy, J.B., Fernández-Suárez, J., Weil, A.B., Franco, M.P., Gonzalo, J.C., 2011. Lithospheric delamination in the core of Pangea: Sm–Nd insights from the Iberian mantle. Geology 39, 155–158.

Hancock, P.L., 1985. Brittle microtectonics: principle and practice. Journal of Structural Geology 7, 437–457.

Heward, A.P., 1978. Alluvial fan and lacustrine sediments from Stephanian-a and Stephanian-b (la Magdalena, Ciñera-Matallana and Sabero) coalfields, northern Spain. Sedimentology 25 (4), 451–488.

Irving, E., Opdyke, N.D., 1965. The palaeomagnetism of the Bloomsburg Red Beds and its possible application to the tectonic history of the Appalachians. Geophysical Journal of the Royal Astronomical Society 9, 153–167.

Johnston, S.T., 2001. The Great Alaskan Terrane Wreck: reconciliation of paleomagnetic and geological data in the northern Cordillera. Earth and Planetary Science Letters 193 (3–4), 259–272.

Julivert, M., Marcos, A., 1973. Superimposed folding under flexural conditions in Cantabrian zone (Hercynian-cordillera, Northwest Spain). American Journal of Science 273 (5), 353–375.

Kollmeier, J.M., van der Pluijm, B.A., Van der Voo, R., 2000. Analysis of Variscan dynamics; early bending of the Cantabria–Asturias Arc, northern Spain. Earth and Planetary Science Letters 181, 203–216.

Lowrie, W., Hirt, A.M., 1986. Paleomagnetism in arcuate mountain belts. In: Wezel-Forese, C. (Ed.), The Origin or Arcs, Developments in Geotectonics. Elsevier, Amsterdam, pp. 141–158.

Lefort, J., 1979. Iberian–Armorican arc and Hercynian orogeny in Western Europe. Geology 7 (8), 384–388.

Macedo, J., Marshak, S., 1999. Controls on the geometry of fold-thrust belt salients. Geological Society of America Bulletin 111, 1808–1822.

Marshak, S., 1988. Kinematics of orocline and arc formation in thin-skinned orogens. Tectonics 7 (1), 73–86.

Marshak, S., 2004. Salients, recesses, arcs, oroclines, and sytaxes - A review of ideas concerning the formation of map-view curves in fold-and-thrust belts. In: Thrust tectonics and hydrocarbon systems: AAPG Memoir 82, 131–156.

Marshak, S., Tabor, J.R., 1989. Structure of the Kingston orocline in the Appalachian fold–thrust belt, New-York. Geological Society of America Bulletin 101 (5), 683–701.

Martinez, F.J., Rolet, J., 1988. Paleozoic metamorphism in the Northwestern Iberian Peninsula, Britanny and related areas in SW Europe. In: Harris, A.L., Fettes, D.J. (Eds.), The Caledonian–Appalachian Orogen, pp. 279–288.

Martínez-Catalán, J.R., 1990. A noncylindrical model for the northwest Iberian allochthonous terranes and their equivalents in the Hercynian belt of Western-Europe. Tectonophysics 179 (3–4), 253–272.

Martínez-Catalán, J.R., Arenas, R., Diaz Garcia, F., Gomez-Barreiro, J., Gonzalez Cuadra, P., Abati, J., Castineiras, P., Fernandez-Suarez, J., Sanchez Martinez, S., Andonaegui, P., Gonzalez Clavijo, E., Diez Montes, A., Rubio Pascual, F.J., Valle Aguado, B., 2007. Implications for the comprehension of the Variscan belt. In: Hatcher Jr., R.D., Carlson, M.P., McBride, J.H., Martínez Catalán, J.R. (Eds.), *4-D Framework of Continental Crust*: Geological Society of America Memoir, p. 200.

Martínez-Catalán, J.R.M., 2002. Variscan–Appalachian Dynamics. Geological Society of America.

Martínez-García, E., 1981. El Paleozoico de la Zona Cantábrica Oriental (Noroeste de España). Trabajos de Geología 11, 95–127.

Merino-Tomé, O.A., Bahamonde, J.R., Colmenero, J.R., Heredia, N., Villa, E., Farias, P., 2009. Emplacement of the Cuera and Picos de Europa imbricate system at the core of the Iberian–Armorican arc (Cantabrian zone, north Spain): new precisions concerning the timing of arc closure. Geological Society of America Bulletin 121 (5–6), 729–751.

Murphy, J.B., Gutierrez-Alonso, G., Nance, R.D., Fernandez-Suarez, J., Keppie, J.D., Quesada, C., Strachan, R.A., Dostal, J., 2006. Origin of the Rheic Ocean: rifting along a Neoproterozoic suture? Geology 34 (5), 325–328.

Muttoni, G., Argnani, A., Kent, D.V., Abrahamsen, N., Cibin, U., 1998. Paleomagnetic evidence for Neogene tectonic rotations in the northern Apennines, Italy. Earth and Planetary Science Letters 154, 25–40.

Pares, J.M., Van der voo, R., Stamatakos, J., Pérez-Estaún, A., 1994. Remagnetizations and postfolding oroclinal rotations in the Cantabrian Asturian arc, northern Spain. Tectonics 13 (6), 1461–1471.

Pastor-Galán, D., Gutiérrez-Alonso, G., Meere, P.A., Mulchrone, K.F., 2009. Factors affecting finite strain estimation in low-grade, low-strain clastic rocks. Journal of Structural Geology 31, 1586–1596.

Pérez-Estaún, A., Bastida, F., Alonso, J.L., Marquinez, J., Aller, J., Alvarezmarron, J., Farias, P., Marcos, A., Pulgar, J.A., 1991. The Cantabrian zone — an interpretation for an arcuate foreland thrust belt. Tectonophysics 191 (3–4), 435.

Pérez-Estaún, A., Bastida, F., Alonso, J.L., Marquinez, J., Aller, J., Alvarezmarron, J., Marcos, A., Pulgar, J.A., 1988. A thin-skinned tectonics model for an arcuate fold and thrust belt — the Cantabrian Zone (Variscan Ibero-Armorican arc). Tectonics 7 (3), 517–537.

Ribeiro, A., Dias, R., Silva, J.B., 1995. Genesis of the Ibero-Armorican arc. Geodinamica Acta 8 (4), 173–184.

Rodríguez-Fernández, L.R., Heredia, N., 1990. Palentine zone structure. Pre-Mesozoic Geology of Iberia. Springer-Verlag, Berlin, pp. 69–71.
Schwartz, S.Y., Van der Voo, R., 1983. Paleomagnetic evaluation of the orocline hypothesis in the central and southern Appalachians. Geophysical Research Letters 10, 505–508.
Stewart, S.A., 1995. Paleomagnetic analysis of fold kinematics and implications for geological models of the Cantabrian/Asturian arc, north Spain. Journal of Geophysical Research-Solid Earth 100, 20079–20094.
Suárez, A., 1988. Estructura del área de Villaviciosa-Libardón (Asturias, Cordillera Cantábrica). Trabajos de Geología 17, 87–98.
Turner, J., Hancock, P., 1990. Relationships between thrusting and joint systems in the Jaca thrust-top basin. Spanish Pyrenees: Journal of Structural Geology 12 (2), 217–226.
Valverde-Vaquero, P., 1992. Permo-Carboniferous magmatic activity in the Cantabrian Zone (N.E. Iberian Massif, Asturias, NW Spain): Boston College, PhD thesis, 1992.
Van der Voo, R., Stamatakos, J.A., Pares, J.M., 1997. Kinematic constraints on thrust-belt curvature from syndeformational magnetizations in the Lagos del Valle Syncline in the Cantabrian Arc, Spain. Journal of Geophysical Research-Solid Earth 102 (B5), 10105–10119.
Van der Voo, R., Channell, J.E.T., 1980. Paleomagnetism in orogenic belts. Rev. Geophys. 18, 455–481.
Weil, A.B., Gutiérrez-Alonso, G., Conan, J., 2010. New time constraints on lithospheric-scale oroclinal bending of the Ibero-Armorican Arc: a paleomagnetic study of earliest Permian rocks from Iberia. Journal of the Geological Society, London 167, 17.
Weil, A.B., Sussman, A.J., 2004. Classifying curved orogens based on timing relationships between structural development and vertical-axis rotations. In: Sussman, A.J., Weil, A.B. (Eds.), Orogenic Curvature: Integrating Paleomagnetic and Structural Analyses: Geological Society of America, pp. 1–16.
Weil, A.B., Van der Voo, R., van der Pluijm, B.A., Pares, J.M., 2000. The formation of an orocline by multiphase deformation: a paleomagnetic investigation of the Cantabria–Asturias Arc (northern Spain). Journal of Structural Geology 22 (6), 735–756.
Weil, A.B., Van der Voo, R., van der Pluijm, B.A., 2001. Oroclinal bending and evidence against the Pangea megashear: the Cantabria–Asturias arc (northern Spain). Geology 29 (11), 991–994.
Weil, A.B., Van der Voo, R., 2002. Insights into the mechanism for orogen-related carbonate remagnetization from growth of authigenic Fe-oxide: a scanning electron microscopy and rock magnetic study of Devonian carbonates from northern Spain. Journal of Geophysical Research-Solid Earth 107 (B4), 14.
Weil, A.B., Yonkee, A., 2009. Anisotropy of magnetic susceptibility in weakly deformed red beds from the Wyoming salient, Sevier thrust belt: relations to layer-parallel shortening and orogenic curvature. Lithosphere 1, 235–256.
Weil, A.B., 2006. Kinematics of orocline tightening in the core of an arc: paleomagnetic analysis of the Ponga Unit, Cantabrian Arc, northern Spain. Tectonics 25, 3.
Whitaker, A.E., Engelder, T., 2005. Characterizing stress fields in the upper crust using joint orientation distributions. Journal of Structural Geology 10 (10), 1778–1787.
Whitaker, A.E., Engelder, T., 2006. Plate-scale stress fields driving the tectonic evolution of the central Ouachita salient, Oklahoma and Arkansas. Geological Society of America Bulletin 118 (5–6), 710–723.
Yonkee, A., Weil, A.B., 2010a. Reconstructing the kinematic evolution of curved mountain belts: internal strain patterns in the Wyoming salient, Sevier thrust belt, U.S.A. Geological Society of America Bulletin 122, 24–49.
Yonkee, A., Weil, A.B., 2010b. Quantifying vertical axis rotation in curved orogens: correlating multiple data sets with a refined weighted least squares strike test. Tectonics 29, 31.